2013-07-03

The Role of SmpB in Licensing tmRNA Entry into Stalled Ribosomes

Mickey R. Miller
Brigham Young University - Provo

The Role of SmpB in Licensing tmRNA Entry into Stalled Ribosomes

Mickey R. Miller

A dissertation submitted to the faculty of
Brigham Young University
in partial fulfillment of the requirements for the degree of

Doctor of Philosophy

Allen R. Buskirk, Chair
Gregory F. Burton
Barry M. Willardson
Emily A. Bates
Joel S. Griffitts

Department of Chemistry and Biochemistry

Brigham Young University

July 2013

ABSTRACT

The Role of SmpB in Licensing tmRNA Entry into Stalled Ribosomes

Mickey R. Miller
Department of Chemistry and Biochemistry, BYU
Doctor of Philosophy

Ribosomes translate the genetic information contained in mRNAs into protein by linking together amino acids with the help of aminoacyl-tRNAs. In bacteria, protein synthesis stalls when the ribosome reaches the 3'-end of truncated mRNA transcripts lacking a stop codon. Trans-translation is a conserved bacterial quality control process that rescues stalled ribosomes. Transfer-messenger RNA (tmRNA) and its protein partner SmpB mimic a tRNA by entering the A site of the ribosome and accepting the growing peptide chain. The ribosome releases the truncated mRNA and resumes translation on the tmRNA template. The open reading frame found on tmRNA encodes a peptide tag that marks the defective nascent peptide for proteolysis. A stop codon at the end of the open reading frame allows the ribosome to be recycled and engage in future rounds of translation.

The entry of tmRNA into stalled ribosomes presents a challenge to our understanding of ribosome function because during the canonical decoding process, the ribosome specifically recognizes the codon-anticodon duplex formed between tRNA and mRNA in the A site. Recognition of proper base-pairing leads to conformational changes that accelerate GTP hydrolysis by EF-Tu and rapid accommodation of the tRNA into the ribosome for peptidyl transfer. The puzzle is that tmRNA enters stalled ribosomes and reacts with the nascent peptide in the absence of a codon-anticodon interaction. Instead, SmpB binding in the decoding center begins the rescue process, but it has been unclear how SmpB licenses tmRNA entry into stalled ribosomes. We analyzed a series of SmpB and ribosomal RNA mutants using pre-steady-state kinetic assays for EF-Tu activation and peptidyl transfer. Although the conserved 16S nucleotides A1492 and A1493 play an essential role in canonical decoding, they play little or no role in EF-Tu activation or peptidyl transfer to tmRNA. In contrast, a third nucleotide, G530, stacks with the side chain of SmpB residue His136, inducing conformational changes that lead to GTP hydrolysis by EF-Tu. A portion of the C-terminal tail forms a helix within the mRNA channel, monitoring the length of mRNA bound in the ribosome to avoid aborting productive protein synthesis. Helix formation in the mRNA channel is essential for accommodation and peptidyl transfer, but not for GTP hydrolysis. We show that conserved residues in the tail are essential for EF-Tu activation, accommodation, or translocation to the P site. Our findings lead to a clearer model of how the tmRNA-SmpB complex enters stalled ribosomes.

Keywords: tmRNA, SmpB, decoding, EF-Tu, ribosome

ACKNOWLEDGEMENTS

I would like to take this opportunity to acknowledge the support of those who have done their best to help me become the scientist that I am still trying to become. First, I would like to thank those friends who have been so helpful in my lab work both for the emotional support as well as the actual work: David Healey, Bailey Savage, Levi Lowry, Joshua Browning, Matt McDowell, Ben Van Leeuwen, Shankar Parajuli, Atin Lamsal, and Diana Valverde.

I also had the great privilege of working with many great graduate students and postdocs in the lab who have provided helpful advice, protocols, reagents, and inspiration; I would like to thank them as well for their patience and support: Chris Woolstenhulme, Jae Yeon Hwang, Andrew Gross, Deanna Cazier, Jacob Crandall, Talina Watts, and Dr. Zhu Liu. I want to give a special thanks to Dr. Douglas Tanner and Dr. Mila Rodriguez-Lopez who were especially helpful and inspirational as I was just beginning.

I wouldn't have been able to accomplish all that I did without Dr. Rachel Green and her lab at Johns Hopkins University School of Medicine. I would like to thank her for allowing me the opportunity to work in her lab learning new techniques and broadening my horizons as a scientist. I am grateful to all of the members of her lab that I had the opportunity to know, but I would especially like to thank Dr. Hani Zaher, Dr. Sergei Djuranovic, Dr. Rodrigo Ortiz-Meoz, Megan McDonald Gilmore, and Beth Rogers for their time, knowledge, and talents which were so influential in moving my work forward. Indeed, I was made to feel a part of Dr. Green's lab each time I was there.

I thank my committee members who have spent so much time reading and evaluating my work. Their insights and advice have been greatly appreciated. I thank my professors as well for the time and effort they put into their lectures for my benefit. I would especially like to express my great appreciation for my advisor, Dr. Allen Buskirk. Of all those that have helped to make me into the scientist that I am becoming, none has had a greater influence than he. Dr. Buskirk taught me how to think like a scientist both by observing his thought process in research as well as by the invaluable opportunities and guidance he gave me to solve problems with my research. It has been a great privilege to work with him.

I would like to acknowledge my family for their love and support. I thank my father, among other things, for the strong work ethic taught to me both by word and by example. I am so grateful to my mother for her listening ears and words of encouragement. I want to express my deep gratitude and love for my dear wife, Carolina. I thank her for her patience and support throughout this stage of my career. She and my two wonderful little girls, Savanah and Victoria, have provided welcome breaks from the rigors of my studies and research. Finally, I must acknowledge my Heavenly Father and thank Him for all of His tender mercies.

TABLE OF CONTENTS

LIST OF TABLES

LIST OF FIGURES

LIST OF ABBREVIATIONS

A site	Aminoacyl tRNA binding site
aa-tRNA	Aminoacylated tRNA
Ala	Alanine
E site	Ribosomal exit site
E. coli	*Escherichia coli*
EF	Elongation factor
fMet	formyl-methionine
GAC	GTPase associated center of ribosome
GDP	Guanosine Diphosphate
GST	Glutathione S Transferase
GTP	Guanosine Triphosphate
His_6	Six-histidine tag
IF	Initiation factor
mRNA	messenger RNA
nt	nucleotide
P site	Peptidyl tRNA binding site of ribosome
Phe	Phenylalanine
PTC	Peptidyl transferase center of ribosome
RF	Release factor
rRNA	ribosomal RNA
S	Svedberg unit
SmpB	Small protein B
T. thermophilus	*Thermus thermophilus*
TLD	tRNA-like domain
tmRNA	transfer-messenger RNA
tRNA	transfer RNA
WT	Wild Type

CHAPTER 1: INTRODUCTION TO RIBOSOMES AND RIBOSOME RESCUE

Ribosomes are large macromolecular machines that synthesize all the proteins within a cell. Without properly functioning ribosomes, cells cannot survive. In fact, ribosomes are the target of many antibiotics that interfere with proper protein synthesis. Translation has been studied extensively and many great discoveries have been made regarding not only its primary role in protein synthesis but also its participation in gene regulation during the translation process. However, there are still several aspects of ribosome function that require more understanding. One of these aspects is the rescue of stalled ribosomes in bacteria. Our research focuses on developing a better understanding of how stalled ribosomes are rescued and will be described in detail after a brief review of ribosome structure and function.

TRANSLATION: AN OVERVIEW

Protein synthesis occurs as ribosomes convert genetic information carried in mRNAs into amino acid sequences of proteins with the help of aminoacyl-tRNA (aa-tRNA). The fully functional prokaryotic ribosome is composed of two subunits. Each subunit is composed of ribosomal RNA (rRNA) and many ribosomal proteins; the rRNA is the larger of the two components, making up more than two-thirds of the ribosome's mass. The large (50S) subunit contains 5S and 23S rRNA whereas the small (30S) subunit contains 16S rRNA. The rRNAs are stabilized by the ribosomal proteins that accompany each subunit. When assembled together, the 50S and 30S subunits form a 70S ribosome complex. Within

the 70S ribosome complex are three binding sites for tRNA: the aminoacyl (A) site, the peptidyl (P) site, and the exit (E) site. Incoming aa-tRNAs are received in the A site, peptidyl-tRNAs bind the P site, and deacylated tRNAs bind the E-site before leaving the ribosome. In each site, tRNAs interact simultaneously with both subunits of the ribosome.

The two subunits play distinct roles in ribosome function. The large subunit contains the peptidyl-transferase center (PTC) and therefore, is primarily responsible for catalyzing peptide-bond formation. It also contains the GTPase associated center (GAC) which is important for regulating the activity of proteins that bind the ribosome reversibly, helping to regulate and promote proper translation. The small subunit functions to ensure proper selection of tRNAs. The region in the small subunit known as the decoding center binds mRNA and determines whether tRNAs entering the ribosome are complementary to the mRNA (Selmer et al. 2006).

Translation by the ribosome is a process comprising three steps: initiation, elongation, and termination (Ramakrishnan 2002; Watson 2008). During initiation, the 30S and 50S subunits must bind onto an mRNA to form an active 70S initiation complex. The ribosome complex then builds a polypeptide one amino acid at a time during elongation with the help of tRNAs and protein cofactors. The ribosome terminates translation when it reaches a stop codon on the mRNA. Release factors and recycling factors are recruited to release the nascent polypeptide and separate the two subunits to recycle them for another round of translation. Each of these steps is described below.

Initiation

To initiate translation in prokaryotes, the 30S subunit binds the three initiation factors IF1, IF2, and IF3. IF3 binds in the E site of the small subunit to prevent reassociation with the large subunit. IF1 binds the A site to prevent binding of aa-tRNAs until the initiation complex is complete. GTP-bound IF2 binds IF1 and reaches into the P site to contact the initiator tRNA, fMet-tRNA^{fMet}. With the initiation factors bound to the small subunit, mRNA and fMet-tRNA^{fMet} can bind as well. The Shine-Dalgarno sequence or ribosome binding site (RBS) of the mRNA binds 16S rRNA. fMet-tRNA^{fMet} and IF2-GTP are then recruited to the P site by the start codon (AUG). The binding of fMet-tRNA^{fMet} to the start codon results in a conformational change in the small subunit that leads to release of IF3. The large subunit is now free to associate with the small subunit leading to GTP hydrolysis by IF2. GDP-bound IF2 as well as IF1 are then released by the ribosome leaving the 70S initiation complex ready for elongation (Watson 2008).

Elongation

Following formation of the initiation complex, the mRNA is read one codon at a time to build the polypeptide through the cyclical process of elongation. In this process, elongation factor Tu (EF-Tu) complexed with GTP delivers aa-tRNAs to the A site of the ribosome. In the decoding center, the ribosome selects a given aa-tRNA based on proper Watson-Crick base pairing between the anticodon of the tRNA and the codon of the mRNA in the A site. The ribosome induces hydrolysis of GTP by EF-Tu following selection of a cognate or complementary aa-tRNA. GDP-bound EF-Tu has low affinity for aa-tRNAs and

therefore releases the aa-tRNA and leaves the ribosome. The aa-tRNA is then accommodated into the A site where it accepts the growing peptide from the peptidyl-tRNA in the P-site through peptidyl transfer in the PTC of the 50S subunit (Watson 2008).

Following peptidyl transfer to the tRNA in the A site, the P-site tRNA is now deacylated. For another round of elongation to occur, the deacylated P-site tRNA must move to the E site, and the A-site tRNA with the growing polypeptide chain must move to the P site. The process by which these tRNAs move within the ribosome is called translocation. GTP-bound elongation factor G (EF-G) enters the ribosomal A site and hydrolyzes GTP. A conformational change in EF-G triggers translocation of the A-site tRNA. Following translocation, the P-site tRNA is now in the E site and the A-site peptidyl-tRNA is now in the P site. EF-G bound to GDP is released by the ribosome as binding affinity has been greatly reduced. The ribosome is now ready for another round of elongation. This cycle continues until the ribosome comes to a stop codon in the mRNA (Watson 2008).

The Mechanism of Decoding

The fidelity of amino acid incorporation into protein during translation results in an error rate of $\sim 10^{-4}$. How does the ribosome maintain this level of fidelity as it discriminates between cognate and near-cognate or non-cognate tRNAs during elongation? Three basic selection stages control the error frequency observed in translation by the ribosome. In the initial selection stage, ribosomes reject incorrect EF-Tu·GTP·aa-tRNA ternary complexes before GTP hydrolysis. Following GTP hydrolysis, the ribosome can still reject near-cognate tRNAs at the proofreading stage (Thompson and Stone 1977; Ruusala et al. 1982; Rodnina

and Wintermeyer 2001). Finally, in a third selection step, the ribosome pre-maturely terminates peptides when a codon-anticodon mismatch occurs in the P site. This is accomplished by recruitment of release factors 2 and 3 to a sense codon following a P-site mismatch (Zaher and Green 2009b).

The decoding mechanism by which the ribosome selects aa-tRNAs is driven by two kinetic discrimination steps that are separated by GTP hydrolysis by EF-Tu (Daviter et al. 2006). After initial binding of the ternary complex to the ribosome through interactions between EF-Tu and ribosomal proteins L7/12 (Kothe et al. 2004; Diaconu et al. 2005), the anticodons of incoming aa-tRNAs begin rapid and reversible sampling of the mRNA in the A-site decoding center (Blanchard et al. 2004; Marshall et al. 2008). The formation of a codon-anticodon duplex that complies with Watson-Crick base pairing leads to local conformation changes of the conserved 16S rRNA nucleotides A1492, A1493, and G530 (Ogle et al. 2001). A1492 and A1493 flip out of helix 44 and G530 rotates from a *syn* to an *anti* conformation to interact with the codon-anticodon helix in the decoding center (Figure 1).

These local conformational changes lead to global conformational changes in the ribosome as the head and shoulder domains of the 30S subunit rotate toward the subunit interface generating the closed form of the ribosome that is essential for tRNA selection (Ogle et al. 2002). The closure of the 30S subunit over the codon-anticodon helix results in a distortion of the tRNA structure (Schmeing et al. 2009; Schuette et al. 2009). These changes in the ribosome and tRNA are then communicated to EF-Tu resulting in activation of EF-Tu followed by GTP hydrolysis. Cognate tRNAs are able to trigger GTP hydrolysis at a

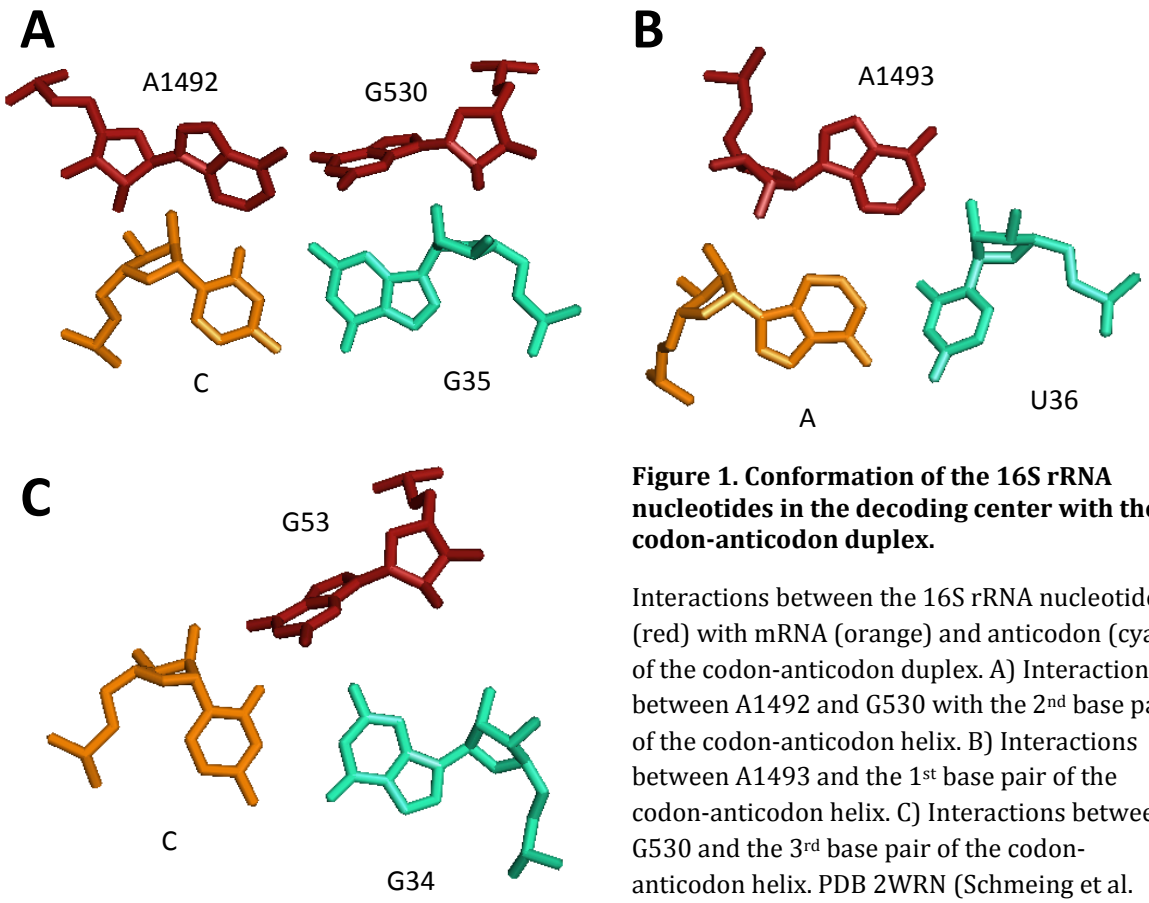

Figure 1. Conformation of the 16S rRNA nucleotides in the decoding center with the codon-anticodon duplex.

Interactions between the 16S rRNA nucleotides (red) with mRNA (orange) and anticodon (cyan) of the codon-anticodon duplex. A) Interactions between A1492 and G530 with the 2nd base pair of the codon-anticodon helix. B) Interactions between A1493 and the 1st base pair of the codon-anticodon helix. C) Interactions between G530 and the 3rd base pair of the codon-anticodon helix. PDB 2WRN (Schmeing et al. 2009).

faster rate than near-cognate and non-cognate tRNAs (Pape et al. 1999; Gromadski and Rodnina 2004). Conversely, near-cognate and non-cognate tRNAs dissociate more readily from the ribosome. EF-Tu activation followed by GTP hydrolysis is the first selective step.

Following hydrolysis of GTP by EF-Tu, the second selective step follows as the aa-tRNA is released from GDP-bound EF-Tu and is fully accommodated into the A site. The 3′ end of the aa-tRNA moves almost 70 Å within the ribosome from its binding site with EF-Tu to the peptidyl transferase center (Stark et al. 2002; Valle et al. 2003a). Again, cognate tRNAs are more rapidly and efficiently accommodated than near-cognate and non-cognate tRNAs (Pape et al. 1999). This second selection step provides an opportunity for proofreading to ensure that a near-cognate or non-cognate tRNA that clears the first

selection step is not accepted in the ribosome afterward. These two selection stages combined with the third selection stage provide the ribosome with the accuracy needed for functional proteins that are essential for the life of a cell.

Termination and Ribosome Recycling

The ribosome continues building a polypeptide until it reaches one of three stop codons (UAG, UGA, and UAA) on the mRNA. Stop codons are recognized by class I release factors (RF) that catalyze hydrolysis of the polypeptide from the peptidyl-tRNA. RF1 recognizes the stop codon UAG, and RF2 recognizes the stop codon UGA. Both RF1 and RF2 recognize the third stop codon, UAA. After the polypeptide is hydrolyzed from the peptidyl-tRNA, a class II release factor in complex with GDP, RF3, binds to the ribosome. Together, the ribosome and class I release factor stimulate the exchange of GDP for GTP within RF3, resulting in a high affinity interaction with the ribosome in the GAC that in turn allows for the release of the class I release factor. Interactions with the GAC stimulate GTP hydrolysis by RF3 returning RF3 to its GDP-bound conformation. In the absence of a class I release factor, RF3 has low affinity for the ribosome leading to its release (Watson 2008).

After the release factors have been released by the ribosome, it must dissociate and release the mRNA and deacylated tRNAs. In order to recycle these ribosomes, ribosome recycling factor (RRF) binds to the A site and recruits GTP-bound EF-G. As seen before in the translocation step, EF-G enters the A site and hydrolyzes GTP. The resulting conformational change stimulates the release of the tRNAs in the P and E sites. Following removal of the tRNAs, GDP-bound EF-G, RRF, and the mRNA are released by the ribosome.

IF3 separates the two subunits leaving an IF3-bound small subunit and a free large subunit ready for another round of translation (Watson 2008).

THE MECHANISM BY WHICH tmRNA RESCUES STALLED RIBOSOMES

Adapted from: Healey D, Miller M, Woolstenhulme C, Buskirk A. 2011. Chapter 29: The mechanism by which tmRNA rescues stalled ribosomes. In *Ribosomes: Structure, Function, and Dynamics* (eds. MV Rodnina, W Wintermeyer, and R Green), pp. 361–373. Springer-Verlag Wien, Vienna, Austria.

Introduction

Not all translation reactions end in the synthesis of a full-length protein. In bacteria, ribosomes stall at the 3′-end of mRNA transcripts lacking stop codons, as they cannot efficiently employ release factors for termination and recycling. Some non-stop mRNAs arise from defects in transcription. RNA polymerase occasionally terminates transcription prematurely; this can occur either as a result of pausing at specific sequences or encountering a tightly-bound protein on the DNA (Abo et al. 2000). Another likely source is the regular process of mRNA degradation. mRNAs are turned over quickly in bacteria, with an average half-life of about six or seven minutes (Bernstein et al. 2002; Selinger et al. 2003). Bacterial mRNAs are degraded by endonucleases and by processive 3′ to 5′ exonucleases (Condon 2007). An exonuclease that collides with a translating ribosome leaves it stalled on the truncated transcript. Ribosome stalling constitutes a serious threat to the integrity of bacterial cells: roughly 1 in 200 translation reactions result in an

irreversible arrest (Moore and Sauer 2005). If these arrested ribosomes were not released, the majority of ribosomes would become inoperative within a single generation.

A translational quality control system in bacteria rescues stalled ribosomes with a small stable RNA known as tmRNA. This remarkable molecule possesses both transfer and messenger RNA activity: aminoacylated with alanine, tmRNA enters stalled ribosomes and adds Ala to the nascent peptide chain (Figure 2). Leaving the broken mRNA, the ribosome resumes translation on the tmRNA template, adding a short tag to the growing polypeptide and terminating translation at a stop codon. The stalled ribosome is recycled and the 11 amino acid tag marks the aborted nascent polypeptide for destruction by cellular proteases (Keiler et al. 1996). Because the ribosome switches templates during protein synthesis, this process is called trans-translation (Figure 2).

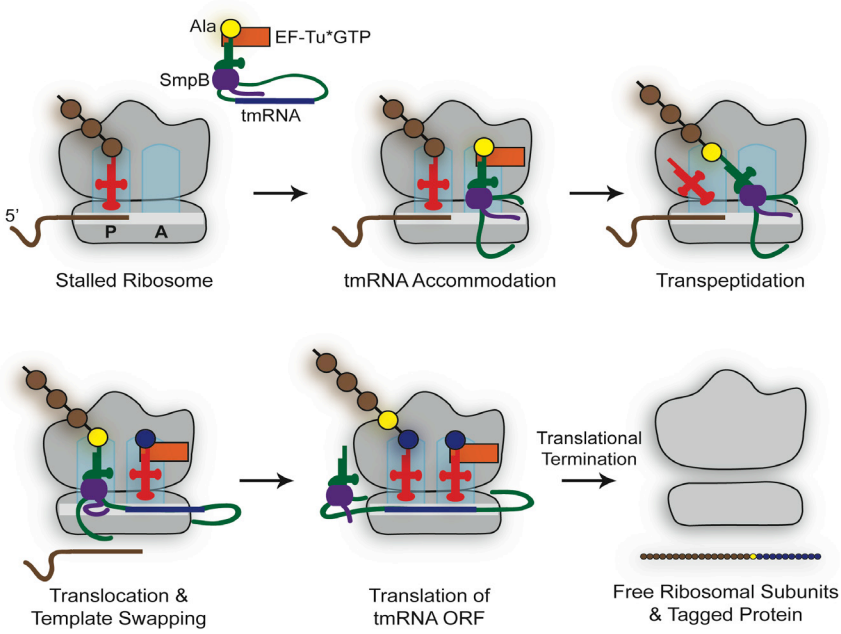

Figure 2. Model of *trans*-translation.

Alanyl-tmRNA (green) and its protein partner SmpB (purple) are delivered to stalled ribosomes by EF-Tu (orange). The nascent polypeptide is transferred to tmRNA. Translocation of tmRNA·SmpB to the P site releases the truncated mRNA and positions the tmRNA ORF (dark blue) in the ribosomal A site. Translation resumes on the tmRNA ORF, directing the addition of an additional ten-residue tag to the nascent polypeptide, after which termination occurs at a stop codon. This process recycles stalled ribosomes, allowing the subunits to dissociate, and tags the nascent peptide for degradation by proteases.

tmRNA and its protein partner, small protein B (SmpB), are found in all fully-sequenced bacterial genomes (Moore and Sauer 2007). tmRNA is essential for viability or pathogenicity in some species of bacteria (Hutchison et al. 1999; Huang et al. 2000), and loss of the tmRNA gene causes sensitivity to various stresses in *E. coli* and *B. subtilis* (Oh and Apirion 1991; Muto et al. 2000). The recycling of stalled ribosomes by tmRNA appears to be its primary function; tagging and destruction of aborted polypeptides appears to be secondary.

Here we review progress in elucidating the mechanism by which tmRNA rescues stalled ribosomes. We examine the molecules involved and the models that have arisen to explain how tmRNA recognizes and enters stalled ribosomes, releases them from truncated transcripts, and tags the proteins for destruction. We also identify and address some of the important mechanistic questions that remain to be answered. Readers interested in the degradation of tagged proteins (Moore and Sauer 2007) or additional biological roles of tmRNA in various bacteria (Keiler 2008) are referred to other recent reviews.

The structure and function of tmRNA

In *E. coli*, tmRNA is the product of a single gene (*ssrA*) that makes a primary transcript 457 nucleotides in length. While in other bacteria, tmRNA levels are regulated by stress responses (Muto et al. 2000), in *E. coli* tmRNA is expressed from a constitutive σ^{70}-like promoter (Oh et al. 1990; Komine et al. 1994). tmRNA is processed at the 5′-terminus by the endonuclease RNase P (Komine et al. 1994). The 3′-terminus is first processed by endonucleases RNase III and/or RNase E, followed by trimming by exonucleases RNase T

and RNase PH (Srivastava et al. 1990; Makarov and Apirion 1992; Li et al. 1998; Lin-Chao et al. 1999). These events are very similar to typical tRNA processing (McClain et al. 1987; Li and Deutscher 2002). Recently tRNAse Z was found to be the primary 3′ endonuclease for normal tRNAs, but it is yet unknown whether tRNAse Z also aids in 3′ processing of tmRNA (Hartmann et al. 2009). The final tmRNA product is 363 nucleotides long and contains a tRNA-like domain (TLD), an mRNA-like domain with an open reading frame (ORF), several helices, and multiple pseudoknot structures (Figure 3) (Chauhan and Apirion 1989; Komine et al. 1994; Williams and Bartel 1996; Felden et al. 1997). tmRNA is resistant to nuclease degradation with a half-life of approximately 60 minutes. It is stabilized by its binding to SmpB—when SmpB is absent, the half-life of tmRNA suffers a four-fold reduction (Hanawa-Suetsugu et al. 2002; Moore and Sauer 2005).

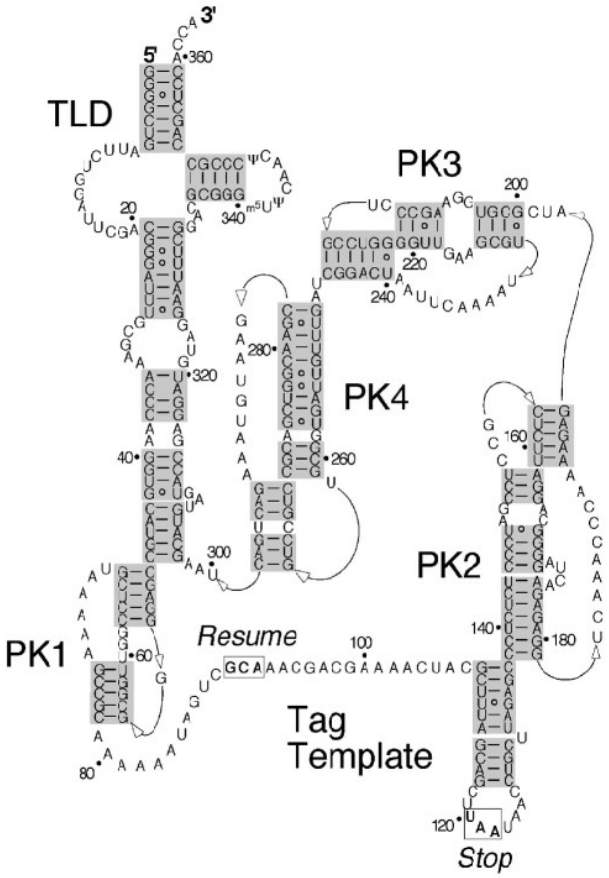

Figure 3. Secondary structure of *E. coli* tmRNA.

The tRNA-like domain (TLD), pseudoknots 1-4, and the open reading frame (including the resume and stop codons) are labeled.

tRNA-like domain

The tRNA-like domain (TLD) is formed through interactions between the mature 5′ and 3′-ends of tmRNA (Figure 3) (Komine et al. 1994). Like tRNA, the TLD contains an acceptor stem ending in 5′-CCA-3′ (Williams and Bartel 1996; Felden et al. 1997; Williams 2000; Zwieb and Wower 2000). This acceptor stem contains a G:U wobble pair that is recognized by alanyl-tRNA synthetase (AlaRS) (Komine et al. 1994; Nameki et al. 1999c). AlaRS is a particularly appropriate synthetase for tmRNA, because tmRNA lacks an anticodon stem, and unlike other synthetases, AlaRS does not need to bind the anticodon region to perform its function (Hou and Schimmel 1988; McClain and Foss 1988).

The tmRNA D loop varies from normal tRNAs in that it lacks dihydrouridine residues (Felden et al. 1998; Hanawa-Suetsugu et al. 2001). It is also much shorter than the traditional D arm and lacks a helical structure. It contains multiple conserved residues that constitute a binding site for SmpB as described below (Barends et al. 2001; Gutmann et al. 2003). The T arm more closely matches its tRNA counterpart (Williams 2000; Zwieb and Wower 2000); it even contains the same modified nucleotides (two pseudouridines and one 5-methyluridine) (Felden et al. 1998). Portions of the D loop interact with the T arm and SmpB to form a central core similar to that found in normal tRNA (Bessho et al. 2007). The T arm and acceptor stem also act as binding sites for elongation factor Tu (Barends et al. 2001; Gutmann et al. 2003; Valle et al. 2003a).

Pseudoknots

Multiple pseudoknot structures exist in tmRNA from all bacterial species (Williams and Bartel 1996; Felden et al. 1997; Williams 2000; Zwieb and Wower 2000). In *E. coli* tmRNA, the four pseudoknots are arranged such that one (PK1) is located upstream of the ORF while PK2, PK3, and PK4 are downstream (Figure 3). Early studies seemed to indicate that PK1 was essential to tmRNA tagging while the other three were dispensable. This was based on the observation that replacing PK1 with a single-stranded motif resulted in severely impaired aminoacylation and tagging, while replacing the other three only marginally reduced tmRNA function (Nameki et al. 1999b; Nameki et al. 2000). It was proposed that PK1 was essential for binding ribosomes in order to position the ORF properly (Nameki et al. 1999a; Valle et al. 2003a).

However, more recent studies have shown that substitution of PK1 with a small, stable hairpin is able to support robust tmRNA tagging ability *in vivo* (Tanner et al. 2006; Wower et al. 2009). These results suggest that the role of PK1 in trans-translation is not ribosome binding, but rather stabilizing the structure of the region between the TLD and the ORF and preventing global misfolding of tmRNA (Tanner et al. 2006; Wower et al. 2009). Pseudoknots 2-4, though certainly less critical than PK1, also play a role in tmRNA function. Pseudoknot 2, 3, or 4 deletion mutants are unable to produce the same levels of mature tmRNA as wild-type (Wower et al. 2004). This finding suggests that PK2, PK3 and especially PK4 play a role in tmRNA maturation, folding, or stability.

Open reading frame

The open reading frame of tmRNA encodes a 10 amino acid tag (ANDENYALAA) that is added to the C-terminus of stalled peptides (Tu et al. 1995). The 5′-end of the tag template is unstructured, providing a site for the ribosome to resume translation, while the 3′-end of this sequence forms part of a conserved helix. A specific tag sequence is not required for the release of stalled ribosomes by tmRNA. The first codon (GCA) can be changed to nearly any other codon without affecting tmRNA function (Williams et al. 1999; O'Connor 2007). The substitution of six histidine residues at the C-terminus of the tag (ANDEHHHHHH) only slightly reduces tmRNA activity (Roche and Sauer 2001). Mutation of the tag sequence, however, can inhibit the proteolytic degradation of the tagged protein (Roche and Sauer 1999; Williams et al. 1999).

In *E. coli*, there are five proteases that degrade tagged proteins: ClpXP, ClpAP, Lon, FtsH and Tsp (Keiler et al. 1996; Herman et al. 1998; Flynn et al. 2001; Choy et al. 2007). The most robust of these, ClpXP, binds to the C-terminus (residues LAA) of the peptide tag (Gottesman et al. 1998; Levchenko et al. 2000; Farrell et al. 2005; Lies and Maurizi 2008). This process is enhanced by an adaptor protein, SspB, that tethers the protease to the tagged peptide by binding both the N-terminal region of the peptide tag (residues AAND) and the ClpX machinery (Levchenko et al. 2000; Flynn et al. 2001). As a result, bacterial cells are able to efficiently recognize and degrade peptide products from rescued ribosomes.

SmpB structure and function

The small, basic protein SmpB is essential to trans-translation; deletion of SmpB conveys all of the same phenotypes characteristic of tmRNA knockouts (Karzai et al. 1999; Dulebohn et al. 2007). SmpB binds tmRNA, enhances its aminoacylation, and prevents its degradation by RNase R (Hanawa-Suetsugu et al. 2002; Shimizu and Ueda 2002; Hong et al. 2005). SmpB also binds to ribosomes and recruits tmRNA; cosedimentation experiments indicate that tmRNA does not bind to ribosomes in the absence of SmpB (Karzai et al. 1999; Hanawa-Suetsugu et al. 2002). There are currently no known functions of SmpB outside of the trans-translation process (Dulebohn et al. 2007).

Structure

The three-dimensional structure of SmpB was solved in solution by NMR (Dong et al. 2002; Someya et al. 2003; Nameki et al. 2005), and the SmpB-tmRNA complex was solved by x-ray crystallography (Figure 4) (Gutmann et al. 2003; Bessho et al. 2007). The crystal structure of the EF-Tu·GTP·tmRNA·SmpB quaternary complex bound to a stalled ribosome was just recently solved as well in *T. thermophilus* (Neubauer et al. 2012). The core is an oligonucleotide binding (OB) fold: six antiparallel β-strands form a closed β-barrel, exposing two highly-conserved RNA-binding sites on opposite sides of the barrel (Dong et al. 2002; Gutmann et al. 2003; Someya et al. 2003). Similar OB-folds have been identified on several other RNA-binding proteins involved in translation, including the initiation factor IF1 (Murzin 1993; Dong et al. 2002). SmpB's β-barrel is enclosed on one side by a long α-helix (Gutmann et al. 2003). Of the 160 amino acids in *E. coli* SmpB, the C-

terminal 30 residues comprise a tail that, while unstructured in solution and not observable in NMR, forms a α-helical structure when bound to the ribosome (Neubauer et al. 2012). The C-terminal tail performs an essential function in *trans*-translation as observed by the fact that deleting the tail abolishes tagging entirely (Sundermeier et al. 2005).

SmpB-tmRNA interactions

SmpB has two separate clusters of highly-conserved amino acids that each function as RNA-binding sites. One of these is a tmRNA-binding site, including E31, L91, N92, and K124. Mutations in these residues dramatically reduce SmpB-tmRNA interaction (Hanawa-Suetsugu et al. 2002; Nameki et al. 2005). SmpB binds tmRNA on the D loop of the TLD region (Gutmann et al. 2003). The binding is specific and has high affinity, with measures of K_d in the low nanomolar range (Karzai et al. 1999; Jacob et al. 2005; Sundermeier et al. 2005; Hallier et al. 2006; Metzinger et al. 2008).

SmpB helps tmRNA mimic the structure and function of alanine-specific tRNA during aminoacylation and entry to the ribosome (Figure 4). As mentioned above, tmRNA's TLD lacks the stem structure of the D stem-loop. SmpB compensates by stabilizing the D

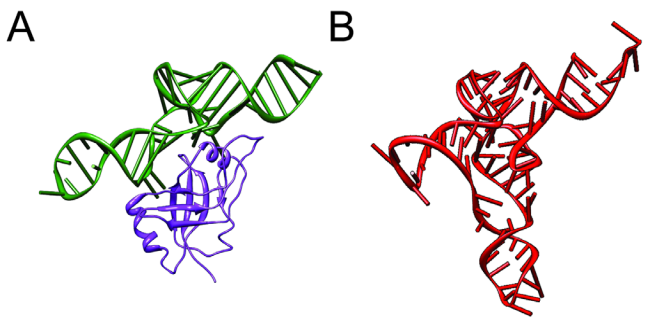

Figure 4. SmpB mimics the anticodon stem-loop of canonical tRNAs.

A) Structure of the tmRNA tRNA-like domain (green) in complex with SmpB (purple) (Bessho et al. 2007) (PDB 2CZJ). B) *T. thermophilus* $tRNA^{Ser}$ is a class II tRNA with an extended variable arm (PDB 1SER). Structures were rendered with Chimera.

loop: residues R45, W118, and V41 interact with tmRNA nucleotides A8 and C48 to form the consecutive stacking structure that is normally formed by C13-G22 base pair in the tRNA D stem (Bessho et al. 2007). SmpB also associates with other conserved tmRNA nucleotides in this region. U17, C18, and A20 in the D loop, as well as U328 and U329 in the T stem, are protected from chemical modification by SmpB (Nameki et al. 2005). Interestingly, the structure of the SmpB-tmRNA complex reveals that SmpB compensates for tmRNA's lack of an anticodon stem-loop. SmpB structurally mimics the anticodon arm of a canonical tRNA (Figure 4) (Bessho et al. 2007), which has important implications for how tmRNA and SmpB enter stalled ribosomes (see below).

How many SmpBs bind to a single tmRNA? The stoichiometry of the tmRNA-SmpB complex has been the subject of some controversy. Optical biosensor and melting curve analysis (Nameki et al. 2005), as well as hydroxyl radical probing (Ivanova et al. 2007), assert that only a single SmpB binds tmRNA. In contrast, enzyme probing, UV crosslinking, footprinting, affinity labeling, and filter-binding assays predict up to three separate SmpB binding sites on tmRNA (Wower et al. 2002; Metzinger et al. 2005). Furthermore, surface plasmon resonance (SPR) indicates that the highest affinity binding site for SmpB is not the TLD but rather a site just upstream of tmRNA's ORF (Metzinger et al. 2008). This second binding site suggests a separate role for SmpB in helping set the reading frame on tmRNA, as discussed below.

SmpB-ribosome binding

Apart from the conserved tmRNA-binding site of SmpB, the protein also has a second site that is likely involved in binding the ribosome during trans-translation. This cluster of highly conserved residues (N17, K18, Y24, Y55, K131, K133, K134, and R139) is located on the opposite side of the β-barrel from the tmRNA binding domain. Mutation of these residues is detrimental to trans-translation activity, but has no effect on tmRNA binding (Dulebohn et al. 2007; Nonin-Lecomte et al. 2009).

Biochemical and structural studies have attempted to localize SmpB in the various steps as it moves through the ribosome. SmpB can interact with both the 30S and 50S subunits of the ribosome (Hallier et al. 2006; Ivanova et al. 2007; Kurita et al. 2007). SmpB footprints are located on the 50S subunit below the L7/L12-stalk (near the GTPase associated center) and on the 30S subunit in the vicinity of the P site. The higher-affinity binding partner appears to be the 30S subunit (Hallier et al. 2006). Hydroxyl radical probing suggests that SmpB helices α1 and α3 contact 16S rRNA in the P site (Kurita et al. 2007); the α1 helix contains some of the conserved residues discussed above. Indeed, the recent crystal structure of the quaternary complex in the ribosome places the α1 helix within binding distance of the decoding center residues, A1492 and A1493 (Neubauer et al. 2012).

Although unstructured in solution, the C-terminal SmpB tail forms an α-helix when bound inside the ribosome (Neubauer et al. 2012). Near the base of the tail, prior to the formation of the helix, Y126 of SmpB (H136 in *E. coli*) base stacks with G530 of the 16S rRNA. Then, starting at roughly D132, the SmpB tail forms an α-helix and extends into the

space of the ribosome normally occupied by mRNA. Two residues in the α-helical tail, V137 and L141 (only one residue, W147, in *E. coli*) appear to make hydrophobic interactions with the surface of ribosomal protein S5.

Two separate pre-accommodation binding sites for SmpB were visualized in cryo-EM structures (Kaur et al. 2006); one SmpB is bound to the 30S A site in the decoding center, the other bound to the GTPase center of the 50S subunit. The 30S-bound SmpB also binds the D loop of tmRNA and has the geometry predicted by modeling the tmRNA-SmpB co-crystal data into the A site of the ribosome complexes, which suggests that this SmpB is functionally relevant (Gutmann et al. 2003; Bessho et al. 2007). The crystal structure of the quaternary complex in the ribosome confirms this model of one SmpB bound to the 30S A site (Neubauer et al. 2012). While the 50S-binding site is consistent with the probing experiments, it does not match the observed co-crystal structure geometry. The conflicting results regarding the number of SmpB binding sites on tmRNA and on the ribosome have led to various models that include more than one SmpB molecule in certain steps of the tagging process.

One SmpB per tmRNA

The controversy regarding the number of SmpB molecules involved in trans-translation has been resolved in favor of a model in which each tmRNA binds a single SmpB both in solution and during its passage through the ribosome. SmpB and tmRNA exist in a 1:1 molar ratio in the cell (Sundermeier and Karzai 2007; Neubauer et al. 2012). Since both get degraded unless they are complexed with the other (Moore and Sauer 2005), this

means that they must be bound together in a 1:1 complex. Accordingly, analysis of complexes isolated from the resumption of translation on tmRNA through termination has found that SmpB and tmRNA are in a 1:1 ratio (Shpanchenko et al. 2005; Bugaeva et al. 2008). Because SmpB replaces the anticodon arm in moving through the ribosome, the predicted binding sites for SmpB in the 30S A and P sites are at their expected locations. The 50S-binding site is likely a biochemical artifact due to SmpB's high basicity. Structural studies now support this model as well; a recent cryo-EM analysis of the post-accommodated state as well as the crystal structure of the pre-accommodated state have only one SmpB bound (Cheng et al. 2010; Neubauer et al. 2012).

Recognition of stalled ribosomes

How are stalled ribosomes recognized by SmpB and tmRNA? It is clear that tmRNA and SmpB do not compete effectively with aminoacyl-tRNAs for binding to elongating ribosomes, as even a 20-fold overexpression of tmRNA and SmpB *in vivo* does not increase the level of tagged proteins (Moore and Sauer 2005). tmRNA is blocked by the presence of downstream mRNA in elongating ribosomes. It was recognized early on that tmRNA only targets ribosomes with truncated mRNA templates (Keiler et al. 1996).

Empty A sites

In vitro experiments with purified components confirm that ribosomes transfer their nascent polypeptides to tmRNA with highest efficiency when there are six or fewer nucleotides in the A site (Ivanova et al. 2004). The rates of peptidyl transfer to tmRNA in

this situation compare roughly to the termination reaction catalyzed by RF1 (Ivanova et al. 2004). Ribosomes bound to longer mRNAs react with tmRNA slightly more slowly, and the efficiency drops 20-fold when the mRNA reaches 15 nt or more in length. Structural work revealed that mRNA nucleotides 12-13 bases downstream of the A site form electrostatic interactions with the highly basic S3, S4, and S5 proteins (Yusupova et al. 2001). This binding may anchor longer mRNAs in the A site and sterically prevent tmRNA and SmpB from binding, while shorter, unanchored mRNAs can loop out into the intersubunit space. In this model, steric occlusion allows tmRNA to distinguish between elongating ribosomes and stalled ones.

The S3, S4, and S5 proteins form a channel between the head and shoulder of the 30S subunit through which mRNA passes as it enters the ribosome (Yusupova et al. 2001). The positive charges that line this channel are expected to create electrostatic repulsion that could open the channel in the absence of mRNA. This open conformation has been seen in some crystal structures (Schluenzen et al. 2000). Possibly the open channel conformation, which would not normally occur with elongating ribosomes, may serve as another recognition element for tmRNA binding (Moore and Sauer 2007). Upon entering the ribosome, the template region of tmRNA must be positioned in this channel for tmRNA to be translated. The channel must open because the 5′ and 3′-ends of tmRNA are paired together—tmRNA is effectively a circular template that cannot be threaded through otherwise. It has not been resolved, however, whether placing the tmRNA template in this channel is involved with recognition of stalled ribosomes or occurs after tmRNA recruitment.

Removal of downstream mRNA

Truncated mRNAs are not the only source of translational stalling; ribosomes can stall in the middle of an mRNA as well. Strings of rare codons in overexpressed transcripts, for example, can stall ribosomes (Roche and Sauer 1999). Similarly, certain nascent peptide sequences can cause the termination or peptidyl transfer reactions to be very inefficient (Hayes et al. 2002a; Hayes et al. 2002b; Collier et al. 2004). If these stalling events persist long enough for the downstream mRNA downstream to be degraded, the ribosomes become irreversibly arrested and have to be rescued by tmRNA (Hayes and Sauer 2003; Sunohara et al. 2004a; Sunohara et al. 2004b; Li et al. 2006). When ribosomes stall in the middle of a transcript, downstream nucleotides must be removed in order for the ribosome to be recycled by tmRNA. The rate of degradation of downstream mRNA is enhanced when the RNA is not protected by translating ribosomes.

The mRNA downstream of the stalling site can be degraded in different ways. Often the mRNA is truncated at the 3′ boundary of the ribosome, about 15 nt downstream from the P-site codon, beyond which 3′ to 5′ exonucleases are sterically blocked (Sunohara et al. 2004a; Li et al. 2006). In some cases, stalling leads to cleavage of the mRNA at the upstream ribosome boundary (Bjornsson and Isaksson 1996; Loomis et al. 2001; Yao et al. 2008), presumably by initial endonucleolytic cleavage.

A site cleavage

Alternatively, in a small number of specific cases, the mRNA is truncated at the A-site codon itself (Hayes and Sauer 2003). This A-site cleavage is probably the result of endonucleases, though this is not formally proven, as no 3′-product of the cleavage event has been detected. The one known A-site endonuclease is the RelE toxin, which cleaves mRNA and inhibits global translation in response to amino acid starvation (Pedersen et al. 2003). It cleaves with some sequence specificity, preferring CAG and UAG codons. Interestingly, it only cleaves RNA within the context of the ribosomal A site; RelE does not cleave RNA by itself (Pedersen et al. 2003). The mechanism of RelE cleavage and its ribosome dependence were clarified recently when the structure of RelE inside 70S ribosomes was solved (Neubauer et al. 2009).

A second A-site endonuclease is postulated to cleave ribosomes stalled during termination after proline codons (Garza-Sanchez et al. 2008). No known nuclease is responsible for this second activity, though it does require the RNase II exonuclease to degrade the downstream RNA to within 21 nt of the P-site codon prior to A-site cleavage (Garza-Sanchez et al. 2009). It has been proposed that the reaction is catalyzed by the ribosome itself (Hayes and Sauer 2003), presumably in a regulated manner, though no such cleavage has been observed in assays using pure components.

Because the *in vitro* studies show that mRNA in the A site inhibits peptidyl transfer to tmRNA, one might expect that A-site cleavage would be essential for tagging to occur. This does not appear to be the case *in vivo*, where the situation is rather more complex. In one example, stalling was reported at a protein ending in Lys-Lys-Arg-Arg sequences (with

rare Arg codons). The tmRNA tag was added immediately after the second Lys codon (Garza-Sanchez et al. 2008). The mRNA was degraded to the 3′-boundary, about 18 nt from the P site, but only very small amounts of A-site cleavage were visible. The authors conclude that 3′-boundary cleavage is sufficient for recruiting tmRNA (Garza-Sanchez et al. 2008). Similar results were found in a separate study on an mRNA with five consecutive rare Arg codons: only boundary cleavage was detected but robust tagging by tmRNA was observed (Li et al. 2006). These data suggest that A-site cleavage may not be essential for tagging to occur *in vivo*, provided that the downstream RNA is processed back to the boundary. Additional experiments will be required to further investigate these discrepancies.

If the ribosome stalls with aminoacyl-tRNA or release factors trapped in the A site, tagging cannot occur; their presence in the A site blocks tmRNA and SmpB binding. This is the case with SecM, a leader peptide that regulates the downstream *secA* gene in response to changing levels of activity in the secretory machinery. When secretory capability is high, the machinery binds the signal peptide in SecM and pulls it out of the ribosome; when the secretory machinery is less active, ribosomes stall at the FxxxxWIxxxxGIRxGP sequence in SecM, changing the mRNA structure and increasing expression of SecA (Nakatogawa and Ito 2002). Inhibition of tagging of stalled SecM is essential to maintaining the logic of the genetic switch. When the ribosome stalls at SecM, Pro-tRNA^{Pro} is bound in the A site as an important part of the stalling mechanism; it also blocks tmRNA-mediated tagging (Garza-Sanchez et al. 2006). Overexpression of SecM or other stalling peptide sequences can lead to tagging as the aminoacyl-tRNAs trapped in the A site are depleted and stalling occurs with no tRNA or release factor blocking the A site.

Entering the A site of stalled ribosomes

Because of its tRNA-like nature, tmRNA is able to interact with elongation factor Tu (EF-Tu) much in the same way as a canonical tRNA does. Reconstructions from cryo-EM show that, on the ribosome, EF-Tu binds the acceptor arm and the T arm of alanyl-tmRNA in a manner virtually identical to that of EF-Tu in complex with aminoacyl-tRNA (Valle et al. 2003a). As with aminoacyl-tRNA, EF-Tu protects the alanyl-tmRNA ester bond from hydrolysis (Rudinger-Thirion et al. 1999; Barends et al. 2000). EF-Tu is likewise essential for the addition of alanine to a stalled peptide by alanyl-tmRNA; peptidyl transfer occurs only at a very slow rate in its absence (Hallier et al. 2004; Shimizu and Ueda 2006).

The hybrid nature of tmRNA, however, raises problems as it enters the ribosome. During normal translation, the signal to accommodate the appropriate tRNA in the A site depends on correct codon-anticodon base pairing between mRNA and cognate tRNA. The ribosome recognizes the geometry of the codon-anticodon base pairs (Ogle et al. 2001; Ogle and Ramakrishnan 2005). As described above concerning canonical decoding, conserved 16S nucleotides A1492 and A1493 flip out of a loop in helix 44 to bind the minor groove of the codon-anticodon duplex (Ogle et al. 2001). G530 also undergoes a *syn* to an *anti* conformational change to interact with the second and third base pairs. These local movements lead to global conformational changes, specifically a rotation of the head and shoulder of the 30S subunit toward the intersubunit space, effectively closing the 30S subunit over the codon-anticodon helix (Ogle et al. 2002). These global conformational

changes are communicated to EF-Tu through its interactions with both of the ribosomal subunits and through distortion of the tRNA structure (Schmeing et al. 2009).

Since tmRNA lacks an anticodon and enters ribosomes that have no mRNA in their A sites, how does it trigger GTPase activity by EF-Tu? Structural and biochemical data suggest that, during ribosome rescue, the decoding center is engaged not by an RNA duplex but by the SmpB protein. In particular, the x-ray crystal structure of the tmRNA-SmpB complex (Figure 4) suggests an interaction between the SmpB tail and the decoding center. Placing the tmRNA-SmpB co-crystal structure into a tRNA-like orientation in the ribosome points the C-terminal tail, roughly 30 residues long, toward the decoding center. Cryo-EM studies of 70S ribosomes bound to tmRNA, SmpB, and EF-Tu in a pre-accommodation complex also orient the C-terminal tail toward the decoding center (Figure 5) (Kaur et al. 2006; Weis et al. 2010b). Indeed, the crystal structure of the pre-accommodation state of the quaternary complex in the ribosomes confirms that SmpB mimics the anticodon stem of tRNA in the ribosome with the tail interacting with the decoding center (Neubauer et al. 2012). Furthermore, computer analysis of the C-terminal tail and hydroxyl radical probing of 16S rRNA with

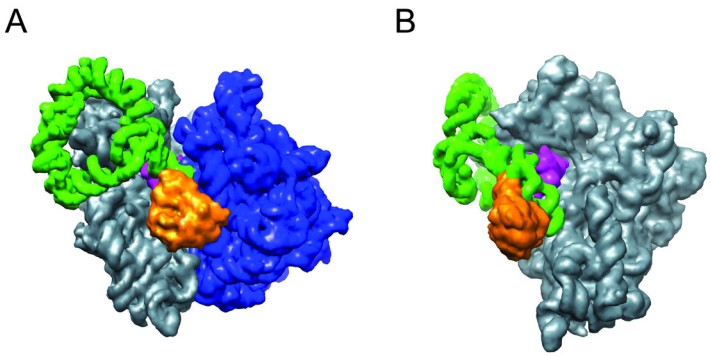

Figure 5. Cryo-EM structure of the pre-accommodation tmRNA·SmpB·EF-Tu complex bound to the 70S ribosome.

A) tmRNA (green) bound to SmpB (purple) (PDB 2OB7) and EF-Tu (orange) (PDB 1OB2) was fitted to the 70S complex using coordinates from Gillet et al. (2007). tmRNA is seen wrapped around the beak of the 30S subunit (grey) with the tmRNA TLD and SmpB bound in the A site. B) Interface view of the 30S subunit shows SmpB bound near the decoding center. Structures were fitted and rendered using Chimera.

SmpB tail residues ligated to Fe-BABE predicted a helical structure for the tail that is confirmed in the crystal structure (Jacob et al. 2005; Kurita et al. 2007; Kurita et al. 2010; Neubauer et al. 2012).

The C-terminal SmpB tail is essential to tmRNA's ability to accept the nascent polypeptide. Mutations of conserved residues in the tail, particularly D_{137}KR, abolish tagging by tmRNA *in vivo* and drastically reduce the rate of peptidyl transfer to tmRNA *in vitro* (Sundermeier et al. 2005). W147 was also shown to inhibit peptidyl transfer (Kurita et al. 2010). At present, no mutations have been found that inhibit EF-Tu activation. Hydroxyl radical and chemical probing experiments have shown that the SmpB tail binds nucleotides in the 30S A site, from the decoding center to the downstream mRNA channel (Kurita et al. 2007). The crystal structure of the pre-accommodated complex specifically shows a base stacking interaction between Y126 of SmpB (H136 in *E. coli*) and the conserved 16S rRNA nucleotide G530 and confirms other interactions with the ribosome in the mRNA pathway that are likely important for allowing the quaternary complex entry into stalled ribosomes (Neubauer et al. 2012). Indeed, SmpB binding to the decoding center protects nucleotides A1492, A1493, and G530 from reacting with chemical probes and causes a shift of these nucleotides in NMR spectra of a small A-site mimic (Nonin-Lecomte et al. 2009). Taken together, the structural and biochemical data suggest a model in which SmpB binding to the decoding center triggers the conformational changes associated with canonical decoding, leading to EF-Tu activation and accommodation of tmRNA. Further work must be performed to determine exactly how the C-terminal tail might trigger those changes and license tmRNA entry into the ribosome.

Template swapping

What is the fate of a truncated mRNA once tmRNA enters the stalled ribosome? The mRNA's binding to the ribosome is stabilized initially by its interaction with the peptidyl-tRNA. After the stalled polypeptide is transferred to tmRNA, the defective mRNA template is ejected with the deacylated tRNA when translocation occurs (Ivanova et al. 2005). *In vivo*, the release of the stalled mRNA may be even faster than observed *in vitro*, as upstream ribosomes may facilitate mRNA release by pulling the loosely bound mRNA free of the leading ribosome (Ivanova et al. 2005). Once the truncated mRNA is released from the stalled ribosome, it is targeted for decay while the ribosome resumes translation on the tmRNA ORF.

Several studies have shown that tmRNA facilitates the degradation of non-stop mRNAs (Yamamoto et al. 2003; Mehta et al. 2006; Richards et al. 2006). Non-stop mRNA decay in bacteria is dependent on SmpB, suggesting that degradation requires the tmRNA-SmpB complex actively to engage stalled ribosomes (Richards et al. 2006). How does tmRNA facilitate the degradation of truncated messages? Once the non-stop mRNA is released from the stalled ribosome, it is no longer protected from exonucleases that efficiently attack the 3′-end of any mRNA lacking secondary structure (Yamamoto et al. 2003). Indeed, the half-life of non-stop mRNAs increases significantly in the absence of tmRNA (Yamamoto et al. 2003; Mehta et al. 2006; Richards et al. 2006). Another possible explanation is that tmRNA may recruit RNase R, a 3′ to 5′ exonuclease, to non-stop mRNAs. RNase R co-purifies with the tmRNA-SmpB complex (Karzai and Sauer 2001), and

mutations in the 3′-end of the ORF reduce non-stop mRNA degradation without affecting the tRNA or mRNA-like functions of tmRNA (Richards et al. 2006).

Selecting the reading frame on tmRNA

As the ribosome switches RNA templates, how is the appropriate codon selected for translation to resume on tmRNA? The transfer of ribosomes to tmRNA resembles a normal round of elongation and not a re-initiation event. No specialized initiator tRNA or protein factors are required, nor does tmRNA base pair with 16S rRNA like the Shine-Dalgarno sequence on mRNA does. It also appears that conserved secondary structural elements in tmRNA do not bind sites on the ribosome to position the first codon in the tmRNA ORF (the resume codon) properly. As discussed above, the four pseudoknots that dominate the tmRNA structure can be replaced with unrelated sequences with little or no loss of tmRNA activity (Nameki et al. 2000; Tanner et al. 2006; Wower et al. 2009). Frame selection does not result from base or structure-specific interactions of tmRNA with the ribosome directly.

tmRNA determinants of frame selection

The tmRNA nucleotides critical for frame selection lie upstream of the resume codon (Williams et al. 1999; Lee et al. 2001; Miller et al. 2008). These two key nucleotides, U85 and A86 in *E. coli*, are conserved in natural tmRNA sequences; A86 was also conserved in random mutagenesis and selection experiments (Williams et al. 1999). Mutations in either base lead to loss of tmRNA function and errors in frame selection *in vitro* and *in vivo*. The U85A mutation, for example, partially shifts translation to the –1 frame (Lee et al.

2001; Miller et al. 2008). Mutation of the universally conserved A86 leads to severe loss of function (Williams et al. 1999; Lee et al. 2001); the A86C mutation shifts translation entirely to the +1 frame (Miller et al. 2008). In contrast, the resume codon itself and the three nucleotides before it can be changed with little or no effect on tmRNA activity (Lee et al. 2001; O'Connor 2007).

U85 and A86 appear to act as markers that cause translation to resume at a given distance downstream. The distance from pseudoknot 1 to U85 is not critical for tagging, but insertions or deletions between A86 and the resume codon (G90) cause misreading of the resume codon (Lee et al. 2001; Miller et al. 2008). Taken together, these mutagenesis data support a model in which U85 and/or A86 bind to a ligand that draws the tmRNA template sequence into the ribosomal A site, placing the nucleotide four bases downstream as the first in the resume codon.

Protein determinants of frame selection

What is the ligand that binds upstream of the resume codon? One candidate that has been proposed is the ribosomal protein S1, which was shown to crosslink to U85 (Wower et al. 2000). Cryo-EM structures of tmRNA bound inside 70S ribosomes reveal that S1 affects the structure of the tmRNA template sequence (Gillet et al. 2007). Though S1 cannot interact directly with tmRNA on the ribosome, it has been proposed that free S1 binds tmRNA and stabilizes a functional, open complex that is then passed to stalled ribosomes (Gillet et al. 2007). In support of this model, one study presents evidence that S1 is required for tmRNA to serve as a template *in vitro* (Saguy et al. 2007). In contrast, two studies using

reconstituted translation systems (Qi et al. 2007; Takada et al. 2007) demonstrated that S1 is non-essential. The only genetic data available likewise argue against a role for S1 in trans-translation (McGinness and Sauer 2004).

A more likely candidate is the SmpB protein. In addition to its well characterized binding site in the TLD, SmpB binds tmRNA upstream of the resume codon, reducing the accessibility of the upstream sequence to nucleases in probing assays (Metzinger et al. 2005). It has been reported that this interaction has a high affinity, comparable to SmpB's binding to the TLD (Metzinger et al. 2008). Intriguingly, mutations in tmRNA that alter frame selection also alter SmpB's interaction with U85 (Konno et al. 2007). While only one SmpB accompanies tmRNA through the ribosome, it seems that SmpB contacts tmRNA at different sites at each step.

Genetic evidence supports the idea that SmpB binding to the upstream region plays a role in frame selection. The A86C mutation in tmRNA leads to the total loss of tagging in the 0 frame and high levels of tagging in the +1 frame. SmpB mutants were identified that suppress both of these defects, restoring activity and proper frame selection on A86C tmRNA (Watts et al. 2009). Intriguingly, the SmpB residues that were mutated (Tyr24, Val129, and Ala130) cluster together in a hydrophobic pocket far away from the TLD binding site. These results demonstrate that SmpB plays a biologically relevant role in setting the frame on tmRNA.

These data are consistent with the following hypothetical structural model. As described above, SmpB acts as an anticodon stem mimic in the SmpB-TLD complex; modeling this structure into the P site of the 70S ribosome shows that residues Tyr24,

Val129 and Ala130 would be found on the A-site face of SmpB, not far from the 16S rRNA and the decoding center. An interaction between this region of SmpB and the tmRNA nucleotides U85 or A86 could draw the tmRNA ORF into the A site. With the first codon (GCA) lying in the mRNA channel in the decoding center, translation would begin with tmRNA as a template. Additional structural and biochemical studies need to be done to rigorously prove this model.

Following tmRNA through the ribosome

Cryo-EM structures of tmRNA and SmpB within the 70S ribosome indicate that the ORF alone lies along the mRNA channel and that pseudoknots 2-4 are organized into a large spiral encircling the beak of the 30S subunit (Valle et al. 2003a; Kaur et al. 2006). The ribosome intersubunit bridges must melt to accommodate the passage of tmRNA through the ribosome. SmpB and tmRNA are translocated together, moving from the A site to the P site and then out through the E site. Although helix H5 unwinds for the 3′-end of the ORF to be decoded, the pseudoknots do not melt during the process (Ivanov et al. 2002). Termination occurs with either release factor binding to the UAA stop codon, after which tmRNA is presumably recycled along with the ribosome subunits.

Future prospects

In the last decade, structural studies have provided new insights into the interaction of the trans-translation machinery with itself and with the ribosome. Together, genetic, structural, and biochemical studies have resolved contradictions in the literature, yielding

models that are well-supported and explain much about how ribosome rescue occurs. They have discovered and emphasized the critical role that SmpB plays in every step of ribosome rescue: stabilizing tmRNA, licensing tmRNA entry into ribosomes, setting the reading frame and moving with tmRNA through the ribosome. However, there are still many unresolved questions: how exactly does SmpB bypass the decoding center to allow accommodation of tmRNA? What signal is transmitted to EF-Tu to hydrolyze GTP? How do SmpB and tmRNA interact to set the reading frame? What is the structure of complexes later in the *trans*-translation process, after SmpB and tmRNA have moved out of the A site? Additional studies need to be done to nail down the answers to these questions.

CONCLUSION

The ribosome utilizes two kinetic discriminatory steps to ensure proper synthesis of proteins encoded by their respective mRNAs. What role do these selection steps play in *trans*-translation? Chapter 2 presents the first kinetic study on ribosome rescue by tmRNA and its protein partner SmpB. We show that the C-terminal tail has an important functional role in licensing tmRNA entry into stalled ribosomes, especially at the accommodation step. Our study also finds that the ribosome does not recognize the rescue machinery by the same mechanism in which it recognizes incoming tRNAs.

In Chapter 3, we show that the SmpB tail does in fact play a role in EF-Tu activation. We provide new insights into how the SmpB tail interacts with the decoding center via biochemical methods. Our work as presented in Chapters 2 and 3 greatly increase our

understanding of this early step in ribosome rescue, namely, the entry of the tmRNA-SmpB rescue machinery into stalled ribosomes.

CHAPTER 2: THE ROLE OF SmpB AND THE RIBOSOMAL DECODING CENTER IN LICENSING tmRNA ENTRY INTO STALLED RIBOSOMES

Adapted from: Miller MR, Liu Z, Cazier DJ, Gebhard GM, Herron SR, Zaher HS, Green R, Buskirk AR. 2011. The role of SmpB and the ribosomal decoding center in licensing tmRNA entry into stalled ribosomes. *RNA*, **17**: 1727–1736.

ABSTRACT

In bacteria, stalled ribosomes are recycled by a hybrid transfer-messenger RNA (tmRNA). Like tRNA, tmRNA is aminoacylated with alanine and is delivered to the ribosome by EF-Tu, where it reacts with the growing polypeptide chain. tmRNA entry into stalled ribosomes poses a challenge to our understanding of ribosome function because it occurs in the absence of a codon-anticodon interaction. Instead, tmRNA entry is licensed by the binding of its protein partner, SmpB, to the ribosomal decoding center. We analyzed a series of SmpB mutants and found that its C-terminal tail is essential for tmRNA accommodation but not for EF-Tu activation. We obtained evidence that the tail likely functions as a helix on the ribosome to promote accommodation and identified key residues in the tail essential for this step. In addition, our mutational analysis points to a role for the conserved K_{131}GKK tail residues in trans-translation after peptidyl transfer to tmRNA, presumably EF-G mediated translocation or translation of the tmRNA template. Surprisingly, analysis of A1492, A1493, and G530 mutants reveals that while these ribosomal nucleotides are essential for normal tRNA selection, they play little to no role in peptidyl transfer to tmRNA. These studies clarify how SmpB interacts with the ribosomal decoding center to license tmRNA entry into stalled ribosomes.

INTRODUCTION

Bacteria contain a conserved quality control system that rescues ribosomes stalled on truncated mRNAs. Arising from premature termination of transcription or from mRNA decay, transcripts lacking a stop codon trap the ribosome at their 3'-ends for prolonged periods. Stalled ribosomes are rescued by transfer-messenger RNA (tmRNA), a stable RNA that acts both as a tRNA and an mRNA. tmRNA is aminoacylated with Ala by alanyl-tRNA synthetase. Together with its protein partner SmpB, tmRNA enters the empty aminoacyl-tRNA site of stalled ribosomes and adds Ala to the growing peptide chain. The ribosome then resumes translation on the tmRNA template, adding a ten amino acid tag to the nascent polypeptide and releasing at a stop codon on tmRNA. This process, known as trans-translation, results in the recycling of stalled ribosomes and the tagging of the aborted polypeptide for degradation by proteases (for a review, see Moore and Sauer 2007).

One unsolved puzzle in the trans-translation model is how tmRNA is allowed to enter stalled ribosomes. Prior to undergoing peptidyl-transfer, an aminoacyl-tRNA must pass through robust decoding mechanisms that exclude tRNAs that cannot form correct codon-anticodon pairs. Because decoding is essential for accurate translation of the genetic code, it has been studied with a variety of tools for many years, and as a result, the selection of tRNAs during canonical translation is well understood (see below). During ribosome rescue, however, codon-anticodon pairing cannot occur because tmRNA lacks an anticodon and binds to ribosomes with little or no mRNA in the A site (Ivanova et al. 2004). While tmRNA entry into stalled ribosomes is not decoding per se, as no genetic information is decoded, tmRNA must somehow trick the decoding machinery into licensing its entry, and

do so without a codon-anticodon interaction. This poses a challenge to our understanding of the trans-translation mechanism and the canonical decoding process.

Canonical tRNA selection involves two kinetic discrimination steps that are separated by the essentially irreversible hydrolysis of GTP (Daviter et al. 2006). Aminoacyl-tRNAs are delivered to the ribosome by EF-Tu. In the first selection step, cognate tRNAs trigger GTP hydrolysis by EF-Tu at a faster rate than non-cognate tRNAs do (Pape et al. 1999; Gromadski and Rodnina 2004); in contrast, non-cognate tRNAs dissociate from the ribosome more readily. Following GTP hydrolysis, the aminoacyl-tRNA is released from EF-Tu, allowing it to be fully accommodated within the ribosome. Accommodation is the movement of the 3'-aminoacylated end of a tRNA from EF-Tu to the peptidyl-transferase center roughly 70 Å away (Stark et al. 2002; Valle et al. 2003b). Cognate tRNAs are more rapidly and efficiently accommodated into the A site than non-cognate tRNAs are (Pape et al. 1999); this is the second selection step.

The faster rates of GTP hydrolysis and accommodation that allow cognate tRNAs to pass these two selection steps arise from conformational changes in the ribosome in response to proper codon-anticodon pairing. Conserved 16S nucleotides A1492 and A1493 flip out of a loop in helix 44 to bind the minor groove of the first and second base pairs in the duplex, as shown in Figure 6A (Ogle et al. 2001; Ogle and Ramakrishnan 2005). G530 also undergoes a conformational change to interact with the second and third base pairs. These local movements lead to global conformational changes, namely a rotation of the head and shoulder of the 30S subunit towards the intersubunit space, effectively closing the 30S subunit over the codon-anticodon helix (Ogle et al. 2002). This change is then

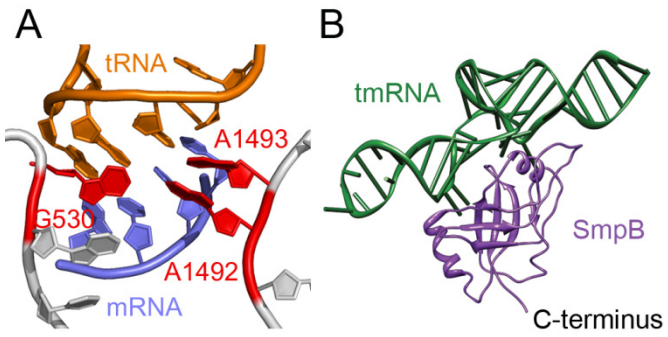

Figure 6. The decoding center and the tmRNA-SmpB complex.

A) Structure of the decoding center showing mRNA (blue) paired with cognate tRNA (orange), and the recognition of this pairing by 16S rRNA nucleotides A1492, A1493, and G530 (red). Created with Pymol from PDB 2J00 (Selmer et al. 2006). B) Co-crystal structure of the tRNA-like domain of tmRNA (green) and SmpB (purple) demonstrating the structural similarity between this complex and a canonical tRNA, where SmpB mimics the anticodon stem. The SmpB C-terminal tail was truncated and would add an additional 27 residues to the C-terminus. Created with Pymol from PDB 2CZJ (Bessho et al. 2007).

communicated to EF-Tu through its interactions with both of the ribosomal subunits and through distortion of the tRNA structure (Schmeing et al. 2009). Mutation of the conserved bases A1492, A1493, or G530 leads to dramatic reductions in the rates of EF-Tu activation and accommodation for cognate tRNAs, leading to error-prone protein synthesis (Cochella et al. 2007).

During the rescue of stalled ribosomes, tmRNA is delivered to the ribosomal A site by EF-Tu (Hallier et al. 2004; Kaur et al. 2006; Shimizu and Ueda 2006). Since it cannot participate in codon-anticodon pairing, tmRNA must use another means to effect EF-Tu activation and accommodation into the A site. Several lines of evidence suggest that during ribosome rescue, the decoding center is engaged not by an RNA duplex but by the SmpB protein. SmpB and the tRNA-like domain of tmRNA form a structure that mimics tRNA (Figure 6B); SmpB acts as the anticodon stem-loop (Bessho et al. 2007). Cryogenic electron microscopy studies of a pre-accommodation complex place SmpB so that the C-terminal tail of SmpB, roughly 30 amino acids long, could be bound in the decoding center (Kaur et al. 2006). Hydroxyl radical and chemical probing experiments have likewise detected interactions of SmpB with ribosomal RNA nucleotides

in the 30S A site (Kurita et al. 2007). Indeed, SmpB binding protects nucleotides A1492, A1493, and G530 from reacting with chemical probes (Nonin-Lecomte et al. 2009).

Taken together, these data support a model in which SmpB acts as a codon-anticodon mimic. By binding the decoding center nucleotides A1492, A1493, and G530, SmpB might trigger the conformational changes associated with canonical decoding, leading to EF-Tu activation and accommodation of tmRNA (Nonin-Lecomte et al. 2009). Currently, this model is supported exclusively by structural and equilibrium binding studies; it has not been determined if these conserved bases in the decoding center are essential for licensing tmRNA's entry into the ribosome. We have tested this model directly, measuring the rates of GTP hydrolysis by EF-Tu and the rate of peptidyl transfer with a series of ribosome and SmpB mutants. Our data show that mutations in the SmpB tail reduce rates of peptidyl transfer to tmRNA, but not GTP hydrolysis by EF-Tu, consistent with a role for the SmpB tail in tmRNA accommodation. We identify key residues in the tail required for this activity and provide evidence that the tail functions as a helix within the ribosome. Surprisingly, analysis of ribosomes containing mutations in A1492, A1493, or G530 reveals that although these nucleotides are essential for both EF-Tu activation and accommodation with normal tRNAs, they play little or no role in licensing tmRNA entry into stalled ribosomes.

RESULTS

Functional importance of conserved residues in the SmpB C-terminal tail

The C-terminal tail of SmpB (residues 131-160 in *E. coli*) is predicted to bind the 30S A site (Kaur et al. 2006; Kurita et al. 2007; Nonin-Lecomte et al. 2009) and deletion of the tail sequence prevents peptidyl-transfer to tmRNA (Sundermeier et al. 2005; Shimizu and Ueda 2006). To identify which residues in the tail sequence are essential for trans-translation, we mutated conserved residues to Ala and assayed SmpB and tmRNA activity *in vivo*. Ribosomes translating a glutathione-S-transferase (GST) construct ending in Glu-Pro-Opal (UGA) stall during termination (Hayes et al. 2002a). These stalled ribosomes were rescued by tmRNA encoding an altered tag, ANDHHHHHHD, that does not target the aborted GST protein for proteolysis (Hayes et al. 2002b). Addition of this tag was detected by anti-His_6 antibodies, indicating completion of all the steps in the trans-translation process. The loss of the anti-His_6 signal on the blot reports on the inhibition of the trans-translation process by the relevant SmpB mutations. GST levels were also monitored to control for protein expression, loading, and blotting. The GST levels are not expected to vary; in the absence of tmRNA activity, ribosomes stalled on the GST template are presumably released by an alternative rescue pathway involving ArfA, allowing GST synthesis by other ribosomes to continue (Chadani et al. 2010).

Analysis of the alignment of 470 SmpB genes (Figure 7) identifies conserved residues that are possible sites of interaction with rRNA, including the D_{137}KR sequence and four partially conserved positive charges at residues 143, 145, 149, and 153 (Andersen et al. 2006). Previously, Karzai and co-workers reported that the D_{137}KR sequence was required for tagging in vivo and for peptidyl transfer to tmRNA (Sundermeier et al. 2005). We confirmed that tagging is lost in the DKR:AAA mutant in our assay (Figure 8B, right). We also tested the relevance of the positively charged residues by replacing Lys143, Arg145, and Arg153 with Ala. (The basic residue at 149 is not conserved in *E. coli*, where it is Val). The triple mutant abolishes tagging activity, while either the double mutant Lys143Ala / Arg145Ala or the single mutant Arg153Ala has no effect (Figure 8B, right), consistent with the notion that at least one of these conserved positively charged residues is absolutely required for SmpB function.

Figure 7. Alignment of the SmpB C-terminal tail.

An alignment of 470 SmpB sequences (Andersen et al. 2006) is displayed as a sequence logo (Crooks et al. 2004). Positively charged residues are highlighted in black. The corresponding *E. coli* sequence (131-160) is shown below. Residues 137-157 are predicted to be helical by the Jpred algorithm (Cole et al. 2008), based on empirical structural propensities and analysis of the multiple sequence alignment.

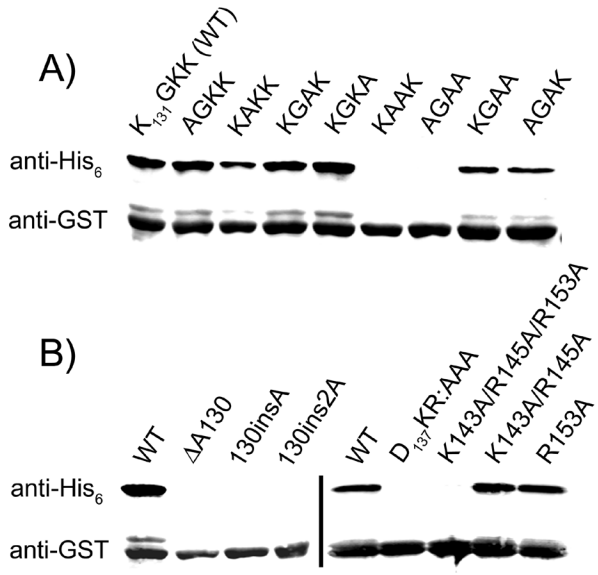

Figure 8. Mutations in the C-terminal tail impair Smpb function.

Various SmpB tail mutants were analyzed for their ability to support tagging of a stalled protein by tmRNA. The complete GST protein with the stalling sequence Glu-Pro-Stop at the C-terminus served as a substrate for tagging. tmRNA was altered to express an ANDHHHHHHD tag; tagging was detected with an anti-His_6 antibody. A GST expression control was visualized on the same blot with anti-GST antibodies. A) Single or multiple Ala mutations reveal essential residues in the conserved K_{131}GKK sequence at the beginning of the tail. B) To study the junction where the tail leaves the body of SmpB, Ala130 was deleted or one or two Ala residues were inserted between Ala130 and Lys131 (left). The roles of three conserved positive charges in the tail and the D_{137}KR sequence were tested by mutagenesis (right).

The alignment also reveals that the K_{131}GKK sequence is highly conserved. Substitution of Gly132 in the K_{131}GKK sequence by Ala resulted in a three-fold reduction in tagging (K_{131}AKK), but no loss of function was observed when the surrounding Lys residues (131, 133 and 134) were substituted, one at a time, with Ala (Figure 8A). When the two residues with the highest conservation, Gly132 and Lys133, were both mutated to Ala together, tagging was no longer detectable (K_{131}AAK). Tagging was also abolished by replacing all three Lys residues with Ala (A_{131}GAA). Mutation of two Lys residues (K_{131}GAA or A_{131}GAK) lowered tagging approximately three-fold. These data point to an important role for Gly132 and suggest that at least one positively charged Lys residue is also essential.

The K_{131}GKK sequence is at the beginning of the C-terminal tail. In the co-crystal structure of the *T. thermophilus* SmpB-tmRNA complex (Bessho et al. 2007), residues corresponding to 131-133 are the last ones seen (the rest of the tail was truncated for

crystallization purposes). Residues 131-133 were seen to exit the body of SmpB at the bottom of the protein, on the opposite side from the tmRNA binding site. To further examine this body / tail junction, we deleted Ala130 or inserted one or two Ala residues between Ala130 and Lys131. Immunoblot analysis revealed that all three of these mutations destroy tagging activity (Figure 8B, left). These observations strongly suggest that the spacing or orientation of the tail is critical for SmpB function as it leaves the body of SmpB.

The helicity and function of the C-terminal tail

The periodicity of basic residues in the SmpB C-terminal tail suggest that the tail, although unstructured in solution, might form an amphipathic helix inside the ribosome. According to our analysis of the tail sequence with the JPred software (Cole et al. 2008), residues 137-157 are likely to form a helix (Figure 7). While the helical propensity of the SmpB tail has been noted for some time (Jacob et al. 2005), it has never been determined whether helix formation plays a role in SmpB function. To address this question, we introduced Pro substitutions to destabilize helix formation in the tail. Several residues from 135-154 were mutated to Pro residues one at a time and tagging was monitored in the immunoblot assay. As a control, corresponding Ala mutants were also tested to ensure that the observed effects result from helix destabilization and not the deletion of essential side chains. None of these Ala mutants reduced tagging (Figure 9A and data not shown), so any observed effects are due to the introduction of Pro.

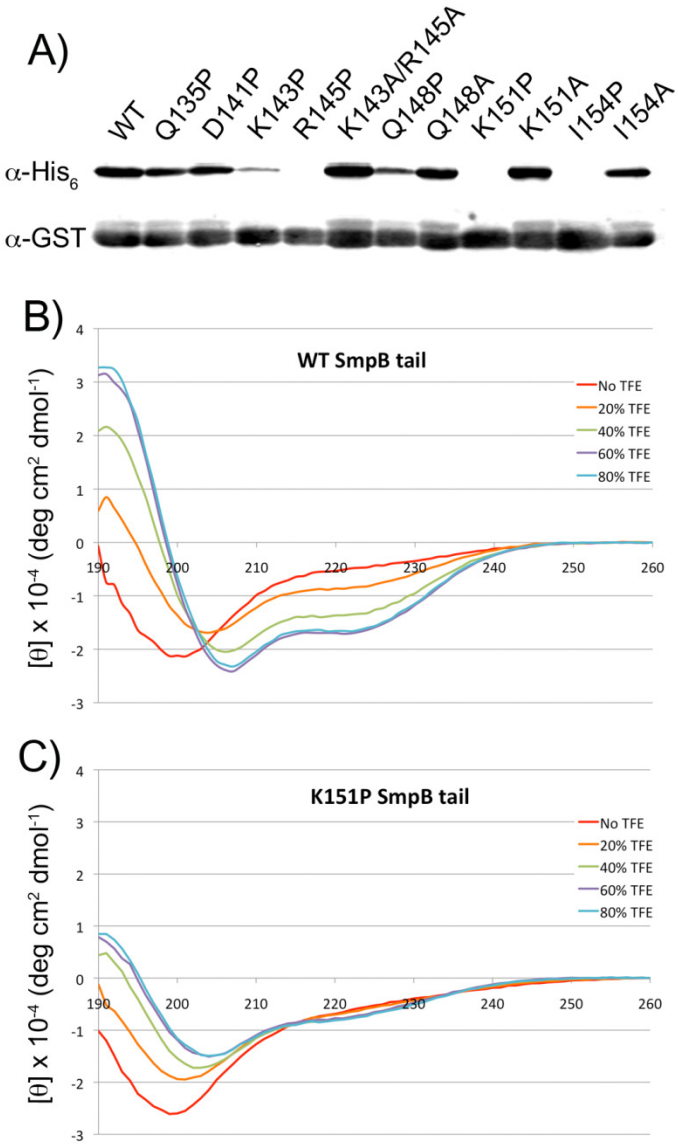

Figure 9. Helicity of the SmpB C-terminal tail.

A) Several residues in the tail were mutated to Pro to destabilize helix formation. The same residues were separately mutated to Ala to control for loss of the original residue. (Only relevant Ala mutants are shown). Addition of the tmRNA-encoded tag was monitored by immunoblot with anti-His_6 antibodies. B) CD spectra of a peptide corresponding to residues 137 to 157 of *E. coli* SmpB (a portion of the C-terminal tail). Trifluoroethanol (TFE) was added at various concentrations to induce secondary structural formation. C) CD spectra of a similar peptide with the Lys151Pro mutation.

Loss of tagging activity in several Pro mutants supports the hypothesis that the SmpB tail forms a helix inside the ribosome to perform its function. Mutation of Lys143, Arg145, Lys151, or Ile154 to Pro reduced tagging to low or undetectable levels, indicating loss of SmpB activity (Figure 9A). In contrast, replacing Gln135 or Asp141 with Pro had little or no effect and the Gln148Pro mutation resulted in only a moderate reduction. These data are consistent with a functional requirement for a helix that spans at least residues 143-154, with a possible break surrounding residue 148.

To further characterize the helicity of the tail sequence, we collected circular dichroism spectra of a short peptide corresponding to

Table 1. α-helical character of peptides corresponding to residues 137-157 of the SmpB C-terminal tail.

SmpB	No TFE	20% TFE	40% TFE	60% TFE	80% TFE
Wild-type	-0.484 ± 0.088	-0.845 ± 0.054	-1.349 ± 0.084	-1.701 ± 0.292	-1.664 ± 0.048
K151P	-0.611 ± 0.101	-0.648 ± 0.215	-0.744 ± 0.025	-0.750 ± 0.104	-0.778 ± 0.135

CD spectra were obtained for each peptide at various concentrations of trifluoroethanol (Figure 6). The minimum at 222 nm is characteristic of α-helices. Standard error is reported. Mean Residue Ellipticity $[\theta]_{222} \times 10^{-4}$.

residues 137–157 (DKRSDIKEREWQVDKARIMKN). As expected, given that the tail is unstructured in solution, the CD spectrum of this peptide in water is consistent with a predominantly random coil conformation (Figure 9B). We added trifluoroethanol (TFE) at concentrations up to 80% to stabilize helix formation. TFE enhances the strength of hydrogen bonds between amides in the peptide backbone (Luo and Baldwin 1997), presumably by decreasing hydrogen bonding to the solvent. In the presence of 40% TFE, the tail peptide exhibits a CD spectrum with α-helical characteristics: a maximum around 190 nm and minima of 208 and 222 nm (Figure 9B). In contrast, the same peptide with a Lys151Pro mutation exhibits spectra characteristic of a random coil, with a minimum around 200 nm, even at 80% TFE (Figure 9C). Quantification of the helical character by comparing the mean residue ellipticity at 222 nm confirms that the Pro mutant has little helical character at any TFE concentration (Table 1). These data demonstrate that the wild type tail peptide has a helical propensity, consistent with earlier predictions. They also show that the Lys151Pro mutation prevents helix formation. Taken together with the finding that the Lys151Ala mutation is tolerated, these studies support our model that loss of helical propensity in the SmpB tail reduces its function *in vivo*.

The SmpB tail is required for peptidyl transfer . . .

While our results show that certain conserved residues in the SmpB tail are essential for tmRNA function *in vivo* and that the tail may function as a helix, they do not reveal which step in the trans-translation process is inhibited by mutating the tail, either peptidyl transfer to tmRNA or engaging the tmRNA template sequence to resume translation. To determine which step is inhibited, we used an *in vitro* assay to further characterize SmpB tail mutants that are inactive *in vivo*. Because we expected that defects in tmRNA entry into the A site were involved, we measured peptidyl-transfer rates to tmRNA using purified components (Figure 10). Ehrenberg and co-workers previously showed that ribosome complexes with fewer than 6 nt in the A site are good substrates for ribosome rescue by tmRNA and SmpB *in vitro* (Ivanova et al. 2004).

We assembled ribosome initiation complexes containing formyl-[^{35}S]Met-tRNA^{fMet} bound to an AUG codon in the P site. Downstream of this start codon, the mRNA sequence contains only a single phenylalanine codon (UUC). The rate of peptidyl transfer was determined by measuring the amount of fMet-Ala dipeptide at various time points after mixing the initiation complex with an excess of quaternary complex composed of Ala-tmRNA, SmpB, EF-Tu, and GTP. As the concentration of the quaternary EF-Tu complex was not saturating in the reaction, the reported rates reflect both binding and catalysis (k_{cat}/K_m).

We measured the rate of dipeptide formation with wild-type SmpB and four SmpB mutants. The K_{131}AAK, D_{137}KR:AAA and Lys151Pro mutants were shown above to abolish tagging in vivo. The Δ153 mutant is truncated at residue 153; Karzai and coworkers showed that deletion of the last seven residues in the tail inhibits tagging in vivo (Sundermeier et al. 2005). The peptidyl-transfer rates of D_{137}KR:AAA, Lys151Pro, and Δ153 were far lower than that of wild-type SmpB (30- to 60-fold, Table 2, left). These results show that conserved residues D_{137}KR are essential for rapid peptidyl transfer to tmRNA and that helix formation is likewise required.

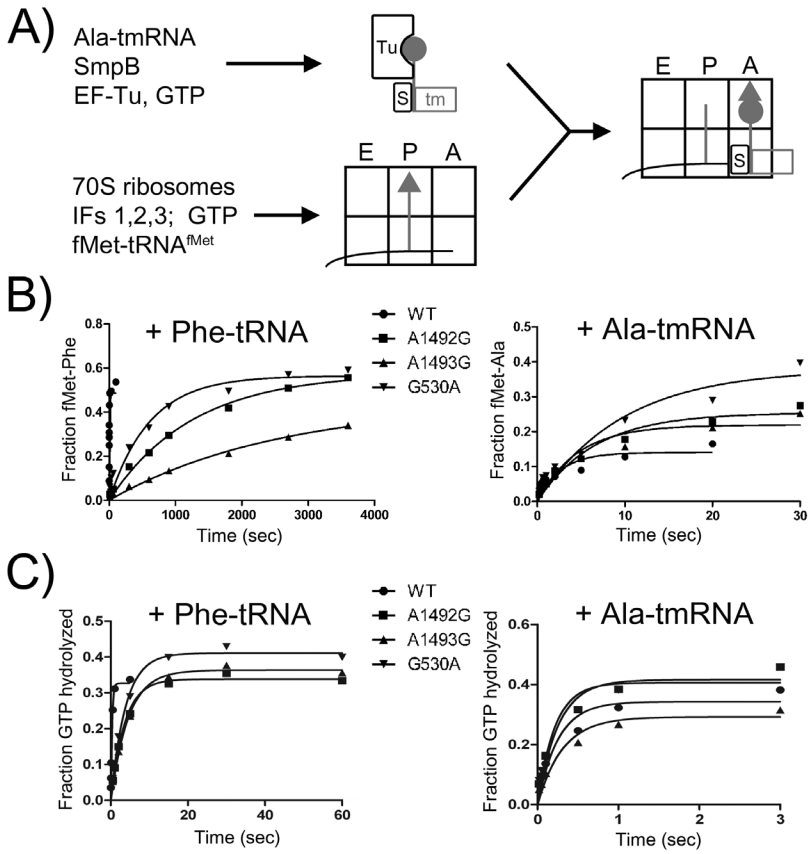

Figure 10. Reaction scheme and representative data for kinetic assays.

A) Reaction scheme for determining GTP hydrolysis and peptidyl transfer rates. The quaternary complex (top) contains EF-Tu, GTP, SmpB, and Ala-tmRNA, and the initiation complex (bottom) contains mRNA, fMet-tRNA^{fMet}, and 70S ribosomes. The mRNA has only a UUC codon in the A site, allowing the initiation complex to react either with Phe-tRNA^{Phe} or Ala-tmRNA. Peptidyl transfer rates are determined by monitoring the rate of formation of the dipeptide fMet-Ala or fMet-Phe using ^{35}S-labeled fMet-tRNA^{fMet}. GTP hydrolysis rates are measured by using [γ-^{32}P]GTP in the quaternary EF-Tu complex and following the appearance of ^{32}P-labeled phosphate upon hydrolysis. B) Representative primary data for dipeptide bond formation rates with Phe-tRNA^{Phe} (left) or Ala-tmRNA (right), with a series of 16S mutants (see also Table 3). C) Representative primary data for GTP hydrolysis rates with Phe-tRNA^{Phe} (left) or Ala-tmRNA (right).

Table 2. Role of the SmpB C-terminal tail.

SmpB	Peptidyl-transfer rate (s^{-1})	GTP hydrolysis rates (s^{-1})
Wild-type	0.29 ± 0.04	8.2 ± 0.6
$G_{132}K$:AA	0.13 ± 0.02	6.0 ± 0.8
Lys151Pro	0.007 ± 0.002	5.3 ± 0.1
Δ153	0.005 ± 0.002	4.5 ± 0.7
$D_{137}KR$:AAA	0.009 ± 0.001	4.6 ± 0.3

Ribosome initiation complexes were reacted with a complex of EF-Tu, GTP, Ala-tmRNA, and SmpB (Figure 7A). Relative rates of dipeptide formation (fMet-Ala) or GTP hydrolysis by EF-Tu were determined for a series of SmpB C-terminal tail mutants. Standard error is reported.

In contrast, we found that the K_{131}AAK mutant supported peptidyl transfer at a rate only two-fold slower than wild-type SmpB (Table 2). This suggests that the K_{131}GKK sequence at the beginning of the C-terminal tail is not essential for tmRNA functions upstream of peptidyl transfer, including activation of EF-Tu or A-site accommodation of tmRNA. To test if these residues were required for tmRNA to serve as a template sequence, we performed a dipeptide reaction, waited until the endpoint was reached, and then added EF-G and Ala-$tRNA^{Ala}$ (the first codon on tmRNA is Ala). In the presence of wild-type SmpB, the tripeptide fMet-Ala-Ala was formed as expected (12% yield, Figure 11). In contrast,

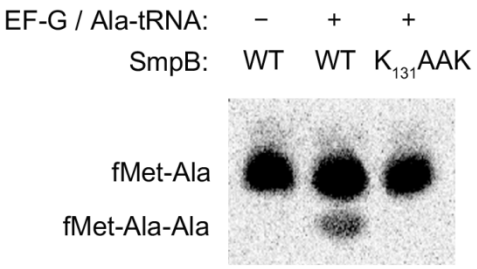

Figure 11. Formation of the tripeptide fMet-Ala-Ala.

The K_{131}GKK sequence in the SmpB tail is required for tmRNA to serve as a template. fMet-Ala dipeptide was formed by reacting initiation complexes with Ala-tmRNA complexes as in Figure 7A. After 5 min, EF-G and Ala-$tRNA^{Ala}$ were added to the reaction and incubated for an additional 10 min. The tripeptide fMet-Ala-Ala is synthesized only if tmRNA is translocated to the P site and the resume codon on tmRNA (Ala) is positioned properly in the A site.

no tripeptide was formed when the reaction was performed with the K_{131}AAK mutant (< 0.5% yield), suggesting that these residues are required for tmRNA to serve as a template.

. . . but not for EF-Tu activation

The peptidyl-transfer assays above do not allow us to distinguish between defects in accommodation and defects in the activation of EF-Tu. As discussed above, structural studies indicate that the C-terminal region of SmpB is positioned in the decoding center prior to the release of tmRNA by EF-Tu (Kaur et al. 2006). As a result, we wondered whether the C-terminal tail is capable of activating EF-Tu, presumably by altering the conformation of key decoding center nucleotides or EF-Tu itself.

Since the activation of EF-Tu is slower than the chemistry of GTP hydrolysis, GTP hydrolysis rates can be used to report on EF-Tu activation as the decoding signal is read in the 30S A site (Pape et al. 1999). GTP hydrolysis rates were determined by mixing initiation complexes with substoichiometric amounts of the quaternary complex composed of Ala-tmRNA, SmpB, EF-Tu, and [γ-^{32}P]GTP. The levels of free radioactive phosphate were monitored at various time points. As expected, no significant GTP hydrolysis was observed in the absence of SmpB (data not shown). Several SmpB mutants were used to test the role of the tail: wild-type, K_{131}AAK, D_{137}KR:AAA, Lys151Pro, and Δ153. Surprisingly, we found that all four SmpB mutants catalyzed GTP hydrolysis very efficiently, less than two-fold slower than wild-type (Table 2, right). Since these SmpB mutants support efficient EF-Tu activation, they must inhibit peptidyl transfer by interfering with the accommodation of tmRNA.

The role of rRNA nucleotides in the decoding center

A1492, A1493, and G530 bind and recognize correctly paired codon-anticodon helices in the A site (Figure 6A) during the canonical decoding process (Ogle and Ramakrishnan 2005). Mutation of these nucleotides results in a dominant lethal phenotype in *E. coli* (Powers and Noller 1990). Anticipating that these nucleotides would also be involved in licensing tmRNA entry during ribosome rescue, we purified ribosomes containing either the A1492G, A1493G, or G530A mutations and measured peptidyl-transfer rates to tmRNA *in vitro*. Mutant ribosomes were purified to homogeneity by an affinity-purification procedure from cells that also express wild-type ribosomes (Youngman and Green 2005; Cochella et al. 2007). The MS2 hairpin was inserted into the mutant 16S rRNA genes, providing a chemical handle for isolation of mutant 30S subunits. In addition to the three decoding center mutants, wild-type MS2-tagged ribosomes were isolated for the wild-type control.

We formed initiation complexes with the MS2-tagged ribosomes and measured the rates of dipeptide formation for either Phe-tRNA^{Phe} or wild-type tmRNA and SmpB. Representative primary data are shown in Figure 10B. Time courses of peptidyl transfer with Phe-tRNA^{Phe} showed that the decoding center mutations led to a ~1000-fold rate reduction (Table 3, left). This is consistent with the reductions in peptidyl-transfer rates reported previously for these mutants (Cochella et al. 2007). In contrast, peptidyl transfer to Ala-tmRNA was reduced by less than two-fold in the A1492G, A1493G, or G530A mutants.

Table 3. The effect of mutations in conserved decoding center nucleotides on canonical translation and *trans*-translation.

	Peptidyl transfer rate (s^{-1})		GTP hydrolysis rate (s^{-1})	
Ribosomes:	Phe-tRNA^{Phe}	Ala-tmRNA	Phe-tRNA^{Phe}	Ala-tmRNA
Wild-type	1.45 ± 0.02	0.29 ± 0.04	3.4 ± 0.1	4.2 ± 0.5
A1492G	0.0008 ± 0.00005	0.16 ± 0.01	0.28 ± 0.009	4.0 ± 0.6
A1493G	0.0005 ± 0.00006	0.23 ± 0.01	0.22 ± 0.003	3.5 ± 0.7
G530A	0.002 ± 0.0002	0.17 ± 0.06	0.26 ± 0.01	4.6 ± 1.0

Tagged ribosomes containing 16S mutations were isolated and used to form initiation complexes. As shown in Figure 7A, these were reacted with complexes containing EF-Tu, GTP, and either Phe-tRNA^{Phe} or Ala-tmRNA and SmpB to determine the relative rate of peptidyl transfer (left) or GTP hydrolysis (right). Representative primary data are shown in Figures 7B and 7C. Standard error is reported.

The fact that mutation of these nucleotides does not significantly reduce peptidyl transfer rates suggests that they do not play an important role in tmRNA accommodation. We were concerned, however, that defects in EF-Tu activation could be masked by the slower, rate-limiting accommodation step. The fact that the SmpB tail is required for accommodation but not EF-Tu activation (as shown above) suggests that the two steps may occur via different mechanisms during ribosome rescue. We therefore analyzed the GTP hydrolysis rates for the decoding center mutants, using both Phe-tRNA^{Phe} and the tmRNA-SmpB complex. Representative primary data are shown in Figure 10C. Time courses of GTP hydrolysis by EF-Tu with Phe-tRNA^{Phe}, used to address canonical decoding, revealed an approximately 15-fold rate reduction in the mutant ribosomes (Table 3, right), consistent with earlier studies (Cochella et al. 2007). In contrast, no rate reduction was seen for the trans-translation reaction with EF-Tu complexed with tmRNA and SmpB. Taken together, these data show that although A1492G, A1493G, and G530A play a critical role in the

canonical decoding process, both in the EF-Tu activation and accommodation steps, they play little to no role in either step as tmRNA enters stalled ribosomes.

DISCUSSION

Stalled ribosomes accept tmRNA into their A sites in the absence of a codon-anticodon interaction. Like canonical tRNAs, Ala-tmRNA is delivered to the ribosome by EF-Tu complexed with GTP. Somehow tmRNA must activate EF-Tu to hydrolyze GTP and release tmRNA into the ribosomal A site, after which it has to swivel into the appropriate conformation for peptidyl transfer to occur. Structural and biochemical studies show that the SmpB protein binds the decoding center in the 30S A site (Kaur et al. 2006; Kurita et al. 2007; Nonin-Lecomte et al. 2009) and that the SmpB C-terminal tail in particular is essential for peptidyl transfer to tmRNA (Sundermeier et al. 2005; Shimizu and Ueda 2006). This function of the tail is independent of SmpB's ability to bind the ribosome or to bind to tmRNA (Sundermeier et al. 2005; Nonin-Lecomte et al. 2009). We have extended these studies by determining the step at which the tail acts during ribosome rescue and identifying characteristics of the tail that are essential for its function.

Our data indicate that the SmpB C-terminal tail is not involved in activating EF-Tu. This is surprising because the tail is positioned such that it could easily interact with decoding center nucleotides or EF-Tu itself to activate GTP hydrolysis. While this work was underway, Himeno and co-workers reported that truncation of the tail does not inhibit GTP hydrolysis by EF-Tu (Kurita et al. 2010). While consistent with our findings, their conclusions were based on the analysis of reaction yields at very long time points (5 and 10

min) and not the comparison of rate constants. This is problematic because they may have overlooked important defects in activity. For example, we found that when reacted with Phe-tRNA, ribosomes carrying the A1493G mutation activated GTP hydrolysis 15-fold slower than wild-type ribosomes. In spite of this defect, the A1493G mutant reached the same endpoint as wild-type ribosomes after only 15 seconds (data not shown). Because Himeno et al. did not obtain rate constants for their SmpB mutants, this kind of defect in GTPase activity cannot be ruled out. By determining rates that were physiologically relevant (on the order of 10 s^{-1}) with pre-steady state kinetic methods that have been used extensively to study canonical decoding, we have ruled out defects in our SmpB tail mutants in activating GTP hydrolysis by EF-Tu.

Our findings support the conclusion that the SmpB tail plays an essential role in the accommodation of tmRNA into the ribosomal A site. Accommodation of the tmRNA/SmpB complex requires both flexibility and significant motion. During the first selection step, canonical tRNAs are conformationally strained. The strain is relaxed as accommodation occurs and the 3'-CCA end moves into the peptidyl transferase center (Ogle and Ramakrishnan 2005). The necessary flexibility is associated with the elbow region of the tRNA (Valle et al. 2003b; Cochella and Green 2005; Schmeing et al. 2009). Does the tmRNA/SmpB complex possess the same flexibility? Only the acceptor stem of tmRNA functions as a tRNA; SmpB acts as the anticodon stem/loop, with their interaction lying just below the elbow region (Figure 6B). It makes sense that the junction between SmpB and tmRNA is right at the position where flexibility is likely to be important. Structural studies suggest that rotation of SmpB is also involved; the tmRNA-SmpB complex rotates 30° during accommodation while remaining bound in the decoding center (Weis et al. 2010a).

Perhaps the interaction of the SmpB tail with the ribosome is required for these motions to occur.

The SmpB tail, although unstructured in solution, may function as a helix inside the ribosomal A site during accommodation. Our Pro-scanning data are consistent with a model in which residues 143-154 function as a helix. The Lys151Pro mutation was found to dramatically reduce the helical potential of the tail peptide and lower the peptidyl-transfer rate 40-fold. The hydroxyl-radical probing studies of Himeno and coworkers also imply a helical structure in the latter half of the C-terminal tail (Kurita et al. 2007). We have added to this work by defining the extent of the helix and demonstrating its functional importance. Helix formation may position key residues in the tail for interaction with elements in the ribosomal A site. Conserved positively charged residues at positions 143, 145, 149, and 153 are likely sites of interaction with rRNA, and their loss inhibits SmpB function. Conserved residues D_{137}KR are also essential for accommodation and may also be a ribosome binding site.

While the SmpB residues discussed above are required for the accommodation of tmRNA into stalled ribosomes, the K_{131}GKK sequence is essential for the translation of tmRNA but not for peptidyl transfer. Two steps occur following the transfer of the nascent peptide to Ala-tmRNA that could be inhibited by mutation of the K_{131}GKK sequence. First, tmRNA and SmpB must be translocated into the P site by EF-G. Hydroxyl radical probing studies by Himeno and co-workers show that when SmpB is bound to the A site, the tail lies along the downstream mRNA path, but that the tail tucks under the body of SmpB when bound to the P site (Kurita et al. 2007). This conformational change moves the tail out of

the way for the tmRNA template to enter the A site. The K_{131}GKK sequence at the beginning of the tail could act as a hinge allowing this movement to occur. A second possibility is that K_{131}GKK affects the placement of the tmRNA template within the decoding center. We previously reported that SmpB plays a role in selecting the reading frame on tmRNA (Watts et al. 2009), a finding later confirmed by structural studies (Fu et al. 2010; Weis et al. 2010a). Residues Tyr24 and Ala130 were implicated in this process; mutation of these residues alters the reading frame on tmRNA. Tyr24 and Ala130 interact where the tail exits the body of the protein at the K_{131}GKK site. Addition or deletion of residues between Ala130 and Lys131 obliterate SmpB function. Whether it is translocation or template placement that is affected, it seems that the angle of exit from the SmpB body and flexibility in the beginning of the tail are critical for SmpB function.

How does SmpB binding in the A site trigger the decoding machinery? Using NMR and chemical probing experiments, Felden and co-workers showed that SmpB binding to ribosomes changes the conformation and reactivity of A1492, A1493, and G530 (Nonin-Lecomte et al. 2009). They concluded that SmpB mimics the codon-anticodon duplex, triggering the same response in the ribosome as cognate tRNA binding does. Our data, however, contradict this model; mutation of these nucleotides has no effect on GTP hydrolysis rates and only very minor effects on the rate of peptidyl transfer to Ala-tmRNA. It appears that A1492, A1493, and G530 do not play a significant role in promoting EF-Tu activation or accommodation of tmRNA. This is striking given their central role in these steps during canonical decoding. Note that our data do not contradict the findings of Felden and co-workers—SmpB binding to nearby nucleotides may alter the conformations of A1492 and A1493 as reported. But the conformational changes in A1492, A1493, and G530

are probably not a result of direct binding by SmpB nor do they have the same functional significance as they do in canonical decoding.

We conclude that SmpB is not a codon-anticodon mimic, strictly speaking, and that SmpB binding to the 30S A site must activate EF-Tu by some other mechanism. This may involve other SmpB-rRNA interactions that account for the majority of binding energy for SmpB in the A site. Alternatively, the S12 protein is known to play an important role in the decoding process and may also influence tmRNA acceptance. S12 mutants can inhibit tmRNA tagging, although their mechanism of action is still unclear (Holberger and Hayes 2009; M Miller and A Buskirk, unpubl.). Experiments to determine the mechanisms by which SmpB activates the decoding machinery will likely yield more insight into trans-translation and perhaps canonical decoding as well.

ACKNOWLEDGEMENTS

This work was supported by grant GM77633 to A.B. and grant GM059425 to R.G. from the National Institutes of Health.

MATERIALS AND METHODS

Circular Dichroism

Peptides corresponding to residues 137-157 of *E. coli* SmpB were purchased from Genscript. The wild-type peptide has the sequence DKRSDIKEREWQVDKARIMKN; the Lys151Pro mutant was also synthesized. CD spectra were recorded on a Avic Model 420 CD

spectrometer in a quartz cuvette with a path length of 0.1 cm. The peptides were dissolved at a concentration of 35 μM and in 10 mM Tris pH 7.5 in the presence or absence on 2,2,2-trifluoroethanol (TFE). The concentrations of TFE varied from 0 to 80% in increments of 20%. Spectra were recorded from 260 nm to 190 nm with 1-nm step size and a time constant of 1.0 s. Data from 3 or 4 replicates were averaged and are reported in mean residue ellipticity. In Table 1, the MRE at 222 nm is reported with the associated standard error.

Immunoblot assays

The pDH210 vector expresses glutathione S-transferase (GST) with the stall-inducing sequence Glu-Pro-Stop at the C-terminus and also expresses tmRNA altered to encode ANDHHHHHHD. SmpB mutants were expressed from derivatives of the pDH113 vector (Watts et al. 2009). Tagging of the GST protein in the presence of the various SmpB mutants was assayed by immunoblotting as described (Tanner et al. 2009).

Expression and purification of MS2-tagged ribosomes

Wild-type and mutant MS2-tagged ribosomes were expressed and purified as described (Youngman and Green 2005; Cochella et al. 2007) with the following modifications. Crude MS2-tagged ribosome pellets were purified over a 15 mL FPLC amylose resin column to which the MBP-MS2-His protein was prebound. Elution was carried out with 10 mM maltose and the eluted ribosomes were concentrated over Amicon Ultra filters (MWCO 100,000, Millipore). Purified ribosomes were depleted of 50S subunits,

so purified MRE600 50S subunits were added back for the formation of initiation complexes.

Purification of translation components

IF1, IF2, IF3 and His-tagged EF-Tu, EF-G, PheRS, and AlaRS were purified as described (Shimizu et al. 2001; Cochella and Green 2005; Brunelle et al. 2006). Formyl-[^{35}S]Met-tRNA^{fMet} was prepared as described (Moazed and Noller 1991). mRNA (GGAAUUCGGGCCCUUGUUAACAAUUAAGGAGGUAUACUAUGUUC) and tRNA^{Ala} were synthesized by T7 transcription of a template assembled by annealing sense and antisense oligonucleotides.

Purification of SmpB

SmpB with an N-terminal His_6-tag was expressed from a pET15b derivative in BL21/DE3 cells. Upon reaching an OD_{600} of 0.5, the cells were treated with 1 mM IPTG for 2 h to induce SmpB expression. The cells were pelleted and resuspended in lysis buffer (20 mM Tris-HCl pH 7.5, 300 mM NaCl, 5 mM imidazole) and cracked using a French press. The lysate was clarified by centrifugation and SmpB was purified on NiNTA agarose resin (Qiagen). Purified SmpB was then dialyzed in SmpB storage buffer (50 mM Tris-HCl pH 6.0, 150 mM NH_4Cl, 200 mM KCl, 5 mM $MgCl_2$, 6 mM β-mercaptoethanol, 50% glycerol).

tmRNA synthesis and aminoacylation

The tmRNA gene was amplified from pKW11 (Roche and Sauer 2001) by PCR, adding the T7 promoter sequence, using the forward primer GAAATTAATACGACTCACTATAGGGGCTGATTCTGGATTCGACGG and the reverse primer TGGTGGAGCTGGCGGGAGTTGAACC. The PCR product was purified and transcribed using the Ambion MEGAshortscript Kit. tmRNA was purified from the reaction by phenol/chloroform extraction followed by ethanol precipitation. tmRNA (5 μM) was aminoacylated with purified AlaRS in buffer 101 (20 mM Tris-HCl, pH 7.5, 20 mM $MgCl_2$, 1 mM DTT), 2 mM ATP, and 10 mM Ala. tmRNA was then purified by phenol/chloroform extraction followed by ethanol precipitation and resuspended in 20 mM KOAc, pH 5.1. The extent of tmRNA aminoacylation was 10-20% as determined by a small parallel reaction with 50 μM [^{14}C]Ala. Likewise, *E. coli* $tRNA^{Phe}$ (Sigma) was aminoacylated with purified PheRS and $tRNA^{Ala}$ synthesized by run-off transcription was aminoacylated by AlaRS.

Peptide-bond formation reactions

70S initiation complexes were formed by incubating 4 μM tagged 70S ribosomes, 10 μM mRNA, 6 μM f[^{35}S]Met-$tRNA^{fMet}$, 5 μM each IF (1, 2, and 3), and 2 mM GTP in buffer A for 45 minutes at 37 °C. Buffer A is 50 mM Tris-HCl, pH 7.5, 70 mM NH_4Cl, 30 mM KCl, 7 mM $MgCl_2$, and 1 mM dithiothreitol (Pape et al. 1999). The complex was purified by layering over a 1.3 mL sucrose cushion (1.1 M sucrose, 20 mM Tris-HCl, pH 7.5, 500 mM NH_4Cl, 10 mM $MgCl_2$, 0.5 mM EDTA) and spun at 258,000 *g* in a TLA100.3 rotor for 2 h. The resulting pellet was resuspended in buffer A, diluted to 100 nM, and aliquots were stored at −80 °C.

The Phe-tRNA^{Phe} ternary complex was prepared by incubating 2 μM charged Phe-tRNA^{Phe}, 8 μM EF-Tu, and 1 mM GTP in buffer A. The tmRNA-SmpB quaternary complexes were prepared by incubating 2 μM charged tmRNA (20 μM total), 40 μM SmpB, 1 mM GTP in buffer A for 5 minutes at 37 °C. 20 μM EF-Tu was added and the reaction mixture was incubated for another 5 minutes at 37 °C.

Peptide bond formation rate reactions were carried out at 37 °C by mixing equal volumes of initiation complexes with either the ternary or quaternary complexes described above. The reactions were stopped at desired time points by addition of KOH to a final concentration of 0.3 M. Reactions with relatively fast rate constants (>0.05 s^{-1}) were performed on a KinTek RQF-3 quench-flow instrument. Reaction products were resolved using cellulose TLC plates in pyridine acetate, pH 2.8, as described (Youngman et al. 2004) and analyzed by autoradiography. The data were fit to a first-order exponential equation with GraphPad Prism5 software. All reported reactions were performed at least twice and the standard error is given.

Tripeptide reactions were performed with an mRNA with a weaker Shine-Dalgarno sequence: GAAGCUGAACGAGAAACGUAAAAUGUAGUAC. Initiation complexes were formed as above and diluted to 100 nM. The Ala-tmRNA quaternary complex was prepared by incubating 5 μM total tmRNA, 15 μM SmpB, 1 mM GTP, and 8 μM EF-Tu for 5 minutes at 37 °C. The quaternary complex was reacted with an equal volume of initiation complex for 5 minutes at 37 °C. The resulting pre-translocation complex was then combined with an equal volume of a solution containing 600 nM Ala-tRNA^{Ala}, 1 mM GTP, and 10 μM EF-G in buffer A, reacted for 10 minutes at 37 °C, and analyzed as above.

GTP hydrolysis reactions

70S initiation complexes were formed as above except non-radioactive fMet-tRNA^{fMet} was used and the complexes were diluted to 500 nM prior to storage at −80 °C. Phe-tRNA^{Phe} ternary complex was prepared by first incubating 20 μM EF-Tu, 17.5 μCi [γ-^{32}P]-GTP (6000 Ci/mmol), 3 mM phosphoenol pyruvate (PEP), and 0.1 mg/ml pyruvate kinase (PK) in buffer A at 37 °C for 30 minutes. Phe-tRNA^{Phe} was then added to 2 μM and incubated on ice for 30 minutes. The tmRNA-SmpB quaternary complexes were prepared by incubating 5 μM tmRNA, 20 μM SmpB (wt or mutant), 20 μM EF-Tu, 17.5 μCi [γ-^{32}P]GTP (6000 Ci/mmol), 3 mM PEP, 0.1 mg/ml PK, 20 mM L-alanine, 2 mM ATP, and 10 μM AlaRS in buffer A at 37 °C for 1 hour. The ternary and quaternary complex mixes were passed through two P30 columns to remove excess [γ-^{32}P]GTP.

GTP hydrolysis rate reactions were carried out on a KinTek RQF-3 quench-flow instrument at 20 °C where equal volumes of initiation complexes and either the ternary or quaternary complexes described above were rapidly mixed and quenched with 40% formic acid at the desired times. Reaction products were resolved on PEI cellulose TLC plates in 0.5 M KH_2PO_4, pH 3.5 and analyzed by autoradiography. The data were fit to a first-order exponential equation with GraphPad Prism5 software. All reported reactions were performed at least twice and the standard error is given.

CHAPTER 3: EF-TU ACTIVATION BY THE tmRNA-SmpB COMPLEX DURING THE RESCUE OF STALLED RIBOSOMES

ABSTRACT

In bacteria, ribosomes stalled on truncated mRNAs are rescued by transfer-messenger RNA (tmRNA) and its protein partner SmpB. After aminoacylated tmRNA and SmpB are delivered to the ribosomal A site by EF-Tu, the nascent peptide is transferred to Ala-tmRNA. During this process, SmpB serves as an anticodon stem mimic that binds the decoding center, licensing tmRNA entry into the ribosome. A recent crystal structure revealed that SmpB residue His136 interacts with G530 of 16S rRNA through a base stacking interaction. Using pre-steady state kinetic methods, we show that disruption of this interaction reduces the rate of GTP hydrolysis by EF-Tu. Other residues in the SmpB tail play supporting roles by positioning His136 properly. Mutation of His136 or deletion of residues 133-160 does not reduce SmpB's affinity for the ribosomal A site. We conclude that the interaction between His136 and G530 plays a functional role in inducing conformational changes in the ribosome that activate the GTPase activity of EF-Tu. Unexpectedly, peptidyl transfer to Ala-tmRNA can be decoupled from GTP hydrolysis. We speculate that GTP hydrolysis is less critical during ribosome rescue because the ribosome does not need to select a specific cognate tRNA, a process that requires irreversible GTP hydrolysis to separate two reversible selection steps, it only needs to prevent tmRNA from aborting the continued translation of intact mRNAs. Taken together, these studies present a clear model of how the tmRNA-SmpB complex enters stalled ribosomes to perform ribosome rescue.

INTRODUCTION

In bacteria, translation of mRNAs lacking a stop codon leads to ribosome stalling at the 3'-end of the transcript. Non-stop mRNAs arise from premature transcriptional termination and mRNA decay. These defective mRNAs pose a particular challenge because bacteria initiate translation on incomplete transcripts and lack the mRNA surveillance mechanisms found in eukaryotes. To rescue stalled ribosomes, bacteria contain an RNA-protein complex made up of transfer-messenger RNA (tmRNA) and its protein partner, SmpB (for reviews, see Moore and Sauer 2007; Janssen and Hayes 2012). tmRNA is aminoacylated with alanine; acting as a tRNA, the tmRNA-SmpB complex enters the A site of stalled ribosomes and adds Ala to the nascent peptide. The ribosome then resumes translation using tmRNA as a template, adding an additional ten amino acids that target the nascent peptide for proteolysis. At a stop codon, the tagged polypeptide is released and the ribosomal subunits are recycled for another round of translation. This process, known as *trans*-translation, tags about 1 out of every 200 proteins for degradation in exponentially growing *E. coli* cells (Moore and Sauer 2005). tmRNA and SmpB are universally conserved in bacteria, are essential for growth in several species (Hutchison et al. 1999; Huang et al. 2000; Thibonnier et al. 2008), inhibits pathogenesis in others (Julio et al. 2000; Okan et al. 2006), and have potential as novel antibiotic targets (Ramadoss et al. 2013).

One question that this model raises is how tmRNA gains entry into stalled ribosomes. Ribosomes discriminate between cognate and non-cognate aminoacyl-tRNAs through robust decoding mechanisms that ensure accurate translation of the genetic code (Zaher and Green 2009a). Cognate tRNAs are selected through two kinetic discrimination steps that are separated by the hydrolysis of GTP by EF-Tu (Daviter et al. 2006). In the first

step, cognate tRNAs trigger GTP hydrolysis by EF-Tu at a faster rate than non-cognate tRNAs do (Pape et al. 1999; Gromadski and Rodnina 2004). The second selection, or proofreading, step occurs after GTP hydrolysis as the aminoacyl-tRNA is released from EF-Tu and undergoes full accommodation within the A site. Cognate tRNAs are accommodated more rapidly than non-cognate tRNAs, which can be rejected prior to peptidyl transfer (Pape et al. 1999).

Cognate tRNAs achieve faster rates in these two selection steps through an induced fit mechanism, as conformational changes in the ribosome occur in response to correct codon-anticodon pairing. At the local level, codon-anticodon pairing is monitored by conserved 16S nucleotides A1492 and A1493, which flip out of helix 44 and bind to the minor groove of the first and second base pairs in the codon-anticodon duplex. G530 also rotates from a *syn* to an *anti* conformation to interact with the second and third base pairs of the duplex (Ogle et al. 2001; Ogle and Ramakrishnan 2005; Schmeing et al. 2009). These local interactions are coupled to global conformational changes that effectively close the 30S subunit over the codon-anticodon helix (Ogle et al. 2002). Mutation of A1492, A1493, or G530 dramatically reduces the rates of EF-Tu activation and peptidyl transfer for cognate tRNAs, leading to lower fidelity in protein synthesis (Cochella et al. 2007).

The canonical decoding mechanism presents a challenge to our current model of *trans*-translation. During ribosome rescue, the decoding center interacts not with an RNA duplex but with tmRNA's protein partner, SmpB. The tmRNA-SmpB complex mimics the structure of a canonical tRNA, with SmpB acting as the anticodon stem loop (Bessho et al. 2007). Given that SmpB binding to the ribosomal decoding center protects the A1492,

A1493, and G530 from reacting with chemical probes (Nonin-Lecomte et al. 2009), we previously tested the model that SmpB's interaction with these key nucleotides might activate GTP hydrolysis through the canonical mechanisms described above. Arguing against this hypothesis, we found that mutation of A1492, A1493, and G530 had little or no effect on the rates of either EF-Tu activation or peptidyl transfer as tmRNA enters stalled ribosomes (Miller et al. 2011).

Reasoning that SmpB must play a key role in licensing tmRNA entry through some alternative mechanism, we also determined the activity of several SmpB mutants. Although we were unable to identify SmpB mutants that inhibit GTPase activation, we found that mutation of key residues in the C-terminal tail of SmpB, residues 132-160, prevents peptidyl transfer to tmRNA (Miller et al. 2011). Coming to similar conclusions, Himeno and co-workers reported that truncation of the SmpB tail after residue 132 abolishes peptidyl transfer but has no effect on GTP hydrolysis rates (Kurita et al. 2010). They also reported that high concentrations of a synthetic peptide corresponding to SmpB residues 133-160 give the same results. By binding in the mRNA channel, this peptide is expected to block positioning of the SmpB tail but not binding of the body of SmpB. Taken together, these studies led to a model in which the C-terminal tail of SmpB is required for accommodation and peptidyl transfer, but not for activation of EF-Tu.

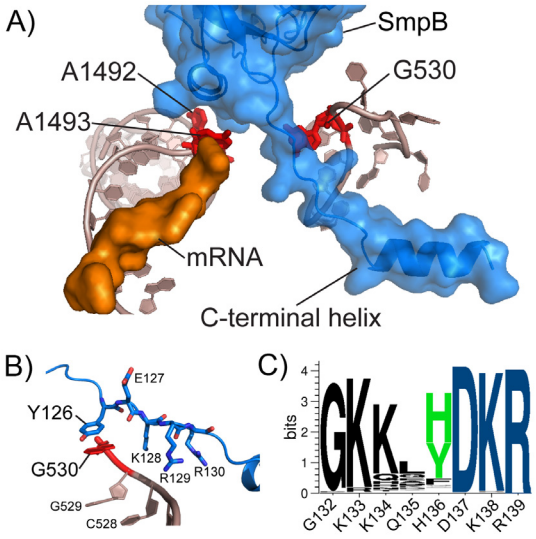

Figure 12. SmpB binding in the ribosomal decoding center.

A) SmpB (blue) engages 16S rRNA nucleotides A1492, A1493, and G530 (red) in the decoding center. The C-terminal tail (residues 132-160) lies in the mRNA channel. Adapted from PDB 4ABR (Neubauer et al. 2012). B) Key *T. thermophilus* SmpB residues interact with G530 and nearby nucleotides. Tyr126 corresponds to His136 in the *E. coli* protein. C) A weblogo of conserved residues in this section of the C-terminal tail is shown with the corresponding residues in *E. coli* SmpB (Andersen et al. 2006).

Here we revisit the question of EF-Tu activation by tmRNA and SmpB in light of the recent crystal structure of these three molecules bound to the 70S ribosome (Neubauer et al. 2012). Using *T. thermophilus* components, Ramakrishnan and co-workers trapped the tmRNA-SmpB complex bound to EF-Tu with the antibiotic kirromycin. The structure reveals in detail how SmpB engages the decoding center (Fig. 12A). Helix 1 binds near A1492 and A1493, which are flipped out of helix 44 of the 16S rRNA, albeit in a conformation that is somewhat different from the conformation seen in canonical decoding. G530 stacks against the side chain of Tyr126. Conserved residues Lys128 and Arg129 bind to the sugar phosphate backbone of G530 and nucleotides nearby, perhaps stabilizing this stacking interaction (Fig. 12B). These structural findings led us to reevaluate the mechanism by which SmpB interacts with the decoding center to license entry of tmRNA into the A site. We report biochemical evidence that the C-terminal tail plays a critical role in EF-Tu activation through a conserved base-stacking interaction with G530, as proposed by Ramakrishnan and co-workers (Neubauer et al. 2012). Surprisingly, we find that peptidyl transfer to tmRNA is decoupled from GTP hydrolysis when the

corresponding residue is mutated, indicating that GTPase activation is less of a selective barrier to tmRNA entry than it is in canonical decoding.

RESULTS

The role of the SmpB C-terminal tail in EF-Tu activation

Himeno and co-workers reported that truncation of the C-terminal tail after residue 132 has no effect on GTP hydrolysis rates (Kurita et al. 2010). One shortcoming in their study, however, is that their GTPase assays involve very long reaction times, so that important defects in activity may have been overlooked. To test the importance of the SmpB tail using pre-steady state kinetic methods, we assembled complexes composed of EF-Tu, GTP, Ala-tmRNA, and SmpB truncated after residue 132. We also assembled initiation complexes containing mRNA with a start codon in the P site, Phe codon in the A site, and no further downstream sequence. This mRNA construct allows us to react these initiation complexes with either tmRNA-SmpB complex or Phe-tRNA^{Phe} for a control. GTP hydrolysis rates were measured by monitoring the appearance of free phosphate over time as [γ-^{32}P]GTP was hydrolyzed by EF-Tu. We found that deletion of the SmpB tail inhibited the GTPase rate by more than 100-fold (Fig. 13B). We also found that addition of a synthetic peptide corresponding to tail residues 133-160 inhibited EF-Tu activation about 80-fold (Fig. 13A). Taken together, these results demonstrate that, contrary to the earlier model, the C-terminal tail of SmpB does play an essential role in EF-Tu activation.

To pinpoint which residues in the SmpB tail induce EF-Tu activation, we created a series of SmpB truncation mutants and analyzed their GTP hydrolysis rates (Fig. 13B). In contrast to the dramatic, more than 100-fold reduction seen when the entire tail is deleted, truncation after residues 139, 146, or 153 resulted in only a modest 6-fold rate reduction of GTP hydrolysis. It appears that one or more residues between Gly132 and Arg139 is essential for activating EF-Tu. An analysis of the alignment of SmpB (Fig. 12C) shows several highly conserved residues in this region of the C-terminal tail. In a previous study (Miller et al. 2011), however, we showed that mutations of the $G_{132}K$ and $D_{137}KR$ sequences had only a modest effect on GTP hydrolysis rates.

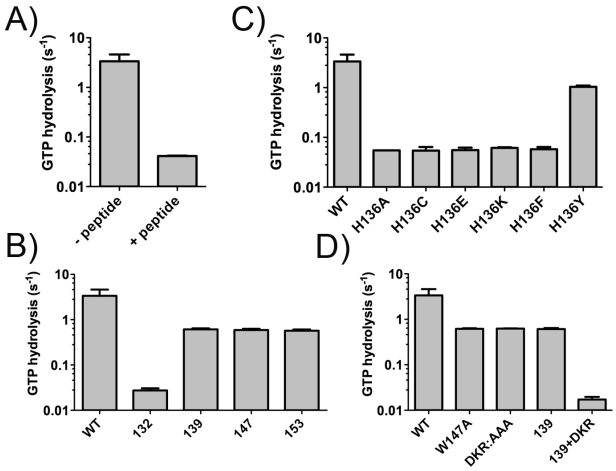

Figure 13. The SmpB C-terminal tail is critical for EF-Tu activation.

GTP hydrolysis rates were measured by reacting complexes containing [γ-^{32}P]GTP, EF-Tu, SmpB, and Ala-tmRNA with 70S initiation complexes, monitoring the appearance of ^{32}P-labeled phosphate upon GTP hydrolysis. A) The reaction was performed in the presence or absence of synthetic peptide corresponding to residues 133-160 of the SmpB tail. In addition, GTP hydrolysis rates were obtained for a series of SmpB proteins: mutants truncated after the residue given (B), single amino acid changes at the residue that stacks on G530, His136 (C), and the D_{137}KR:AAA and 139 truncatation mutations alone and in combination (D). Standard error is given.

His136 in SmpB plays a role in EF-Tu activation

In the recent crystal structure of *T. thermophilus* tmRNA, SmpB, and EF-Tu bound to the ribosome (Neubauer et al. 2012), SmpB residue Tyr126 stacks with G530 of 16S rRNA.

This residue is conserved as His or Tyr, the side chains best able to participate in base-stacking interactions. To test the importance of this stacking interaction, we mutated the corresponding residue in *E. coli*, His136, to Ala and measured the rate of GTP hydrolysis by EF-Tu. This single mutation led to a nearly 70-fold reduction in the rate of GTP hydrolysis (Fig. 13C). Similar defects were seen with the polar amino acids Cys, Lys, and Glu. Although a few species have the aromatic side chain Phe at this position, we found that the His136Phe mutation caused the same rate defect as the His136Ala. In contrast, the His136Tyr mutation reduced the rate only ~3-fold. The fact that the His136Tyr mutant activates EF-Tu lends support to the structural finding that His136 interacts with the decoding center by stacking with the base of G530.

In a previous study (Miller et al. 2011), we showed that the G530A point mutation in 16S rRNA had no effect on EF-Tu activation by the tmRNA-SmpB complex. In an attempt to further disrupt the base stacking interaction, we purified MS2-tagged ribosomes containing the G530U mutation and measured GTP hydrolysis rates (Fig. 14). As expected, this mutant inhibits EF-Tu activation during canonical decoding as seen by the significant rate reduction with Phe-tRNA^{Phe}. When reacted with the tmRNA-SmpB complex, however, the rate of GTP hydrolysis is not significantly reduced by the

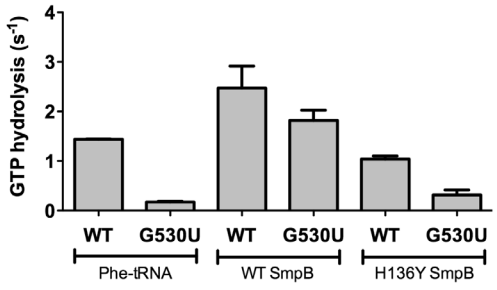

Figure 14. Synergistic effects between G530 and His136 mutants are consistent with a stacking interaction between them.

GTP hydrolysis rates were measured for EF-Tu complexes containing either Phe-tRNA^{Phe} or Ala-tmRNA complexed with either wild type or His136Tyr SmpB. These complexes were reacted with initiation complexes formed with either wild type or G530U tagged mutant ribosomes. Standard error is given.

G530U mutation. When we used the His136Tyr SmpB mutant, we observed an 8-fold reduction in the rate of GTP hydrolysis in combination with the G530U mutant ribosomes (Fig. 14). The synergistic effect observed when these two mutants react is consistent with their affecting the same interaction in EF-Tu activation. Taken together, these studies support a model in which base stacking between His136 and G530 is essential for efficient GTP hydrolysis by EF-Tu in stalled ribosomes.

Other residues in the SmpB tail play supporting roles in EF-Tu activation

The results from the 139, 147, and 153 truncation mutants suggest that other residues in the tail play at least a supporting role in EF-Tu activation. The C-terminal tail of SmpB forms an α-helix as it binds in the mRNA channel of the ribosome (Miller et al. 2011; Neubauer et al. 2012). Several interactions between the SmpB tail and 16S rRNA that were observed close to Tyr126 in *T. thermophilus* SmpB led us to hypothesize that these interactions might help position His136 in *E. coli* for its stacking interaction with G530. In an effort to determine other SmpB residues that might contribute to efficient EF-Tu activation, we characterized two other SmpB mutants. The *T. thermophilus* equivalent to Trp147 in *E. coli*, Val137, appears to be involved in hydrophobic interactions with the surface of ribosomal protein S5 (Neubauer et al. 2012). Himeno and co-workers reported that the Trp147Cys mutant had defects in peptidyl transfer but not EF-Tu activation (Kurita et al. 2010). We made the Trp147Ala mutant and measured the GTP hydrolysis rate by EF-Tu. This mutation lowered the GTP hydrolysis rate by 6-fold (Fig. 13D), the same

amount as truncations after 139, suggesting that disruption of this hydrophobic interaction with S5 has the same effect as deleting these residues involved in helix formation.

In the *T. thermophilus* structure, two basic residues adjacent to Tyr126, Lys128 and Arg129, form ionic bonds with the sugar-phosphate backbone near G530 of 16S rRNA as shown in Fig. 1A (Neubauer et al. 2012). Although these residues are highly conserved, they play only a minor role in EF-Tu activation: mutation of the corresponding *E. coli* residues D_{137}KR to AAA only has a 6-fold effect (Fig. 13D). In the context of the 139 truncation, however, the DKR to AAA mutation decreases the rate of GTP hydrolysis more than 100-fold. This level of activity is similar to what we observed with the tail fully deleted in the 132 truncation mutant. We conclude that Lys138 and Arg139 assist in EF-Tu activation but that their importance is masked by redundant mechanisms, especially the interaction of residues downstream of DKR within the mRNA channel, where Trp147 binds to ribosome protein S5. We speculate that these interactions together stabilize and position His136 to interact with G530.

Mutations in the SmpB tail do not reduce ribosome binding affinity

To test if the reduction in GTPase rates in the SmpB mutants results from impaired ribosome binding in the A site, we used a fluorescence-binding assay to measure the apparent affinity of SmpB for stalled ribosome complexes. Rodnina and coworkers have used aminoacylated tRNAs labeled with various fluorophores to monitor changes in tRNA structure in the ribosome (Rodnina et al. 1996). Structural changes produce altered fluorescence emissions as the environment of the fluorophore changes. We reacted

ribosome initiation complexes with Phe-tRNA^{Phe} labeled with proflavin and EF-G, generating ribosome complexes with labeled fMet-Phe-tRNA^{Phe} in the P-site. We then added wild type SmpB, the 132 truncation mutant, or the His136Ala mutant and monitored changes in fluorescence (Fig. 15A). From the fluorescence data, we were able to calculate apparent dissociation constants (K_d) for each of the SmpB proteins (Fig. 15B). Neither the 132 truncated SmpB nor the His136Ala mutant show defects in binding to stalled ribosomes. These data agree with earlier reports (Sundermeier et al. 2005; Nonin-Lecomte et al. 2009) that the C-terminal tail is not required for high-affinity binding. These data support the conclusion that His136 is not essential for ribosome binding per se but for activation of EF-Tu.

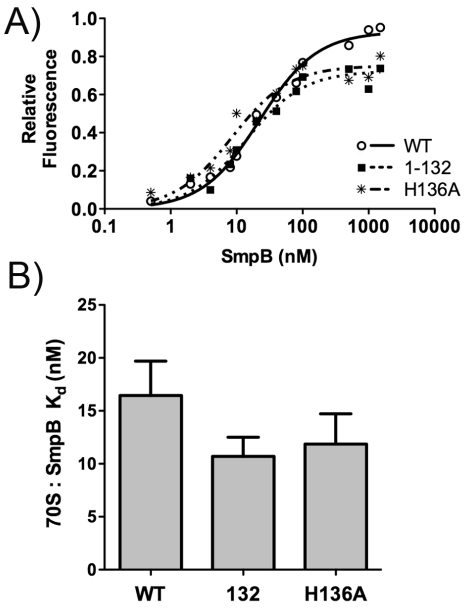

Figure 15. Binding of SmpB to stalled ribosome complexes.

A) Representative data showing the normalized fluorescence of P-site-bound proflavine-labeled fMet-Phe-tRNA^{Phe} upon SmpB binding. B) Apparent dissociation constants were determined from the fluorescence data for wild type SmpB and two SmpB tail mutants. Each experiment was performed at least six times. Standard error is given.

Release of tmRNA from EF-Tu can be decoupled from GTP hydrolysis

Our data indicate that the C-terminal tail is essential for both EF-Tu activation and for peptidyl transfer. In a previous study, we found that the D_{137}KR : AAA mutation inhibits peptidyl transfer, as do mutations that prevent the tail from forming a helix within the

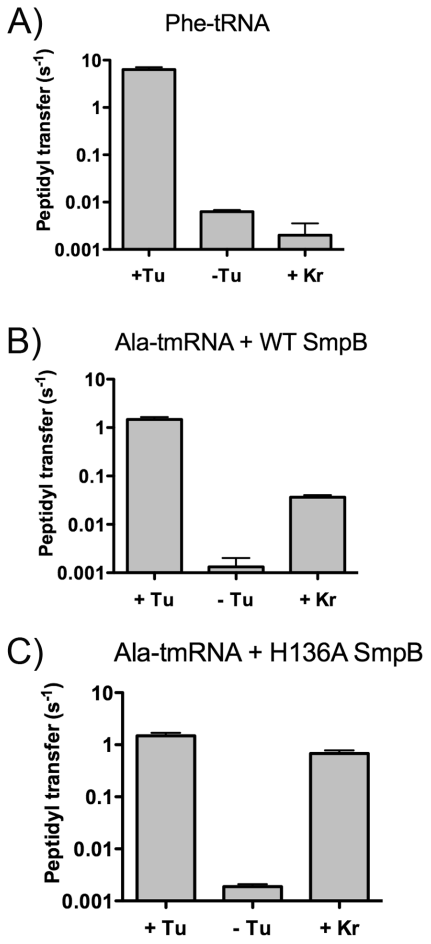

Figure 16. Peptidyl transfer to tmRNA can be separated from GTP hydrolysis by EF-Tu.

Rates of dipeptide bond formation were determined using ^{35}S-labeled fMet-tRNA^{fMet} under three conditions: with EF-Tu, without EF-Tu, and with EF-Tu and 200 μM kirromycin (Kr). Reactions were performed under these three conditions using Phe-tRNA (A) and Ala-tmRNA together with wild-type (B) and His136Ala SmpB (C). Standard error is given.

mRNA channel. To test the importance of His136 in peptidyl transfer, we reacted initiation complexes containing formyl-[^{35}S]-fMet-tRNA with saturating concentrations of Ala-tmRNA and wild-type or His136Ala SmpB. Unexpectedly, the rates of peptidyl transfer were equivalent for the wild-type and mutant SmpB (compare +Tu rates in Fig. 16B and 16C). This is surprising because mutation of the D_{137}KR sequence immediately downstream strongly inhibits peptidyl transfer (> 30-fold). Moreover, the rate of peptidyl transfer with the His136Ala mutant (1.5 ± 0.2 s^{-1}) is faster than the rate of GTP hydrolysis (0.05 ± 0.00005 s^{-1}). In canonical decoding, GTPase activation is essential for release of the tRNA from EF-Tu prior to accommodation and peptidyl transfer. With this SmpB mutant, however, even though GTP hydrolysis is slow, it is not rate-limiting. It appears that peptidyl transfer to tmRNA with the His136Ala mutant can be decoupled from GTP hydrolysis.

EF-Tu's role in *trans*-translation is somewhat unclear: although it binds tmRNA and delivers it to the ribosome (Barends et al. 2001; Valle et al. 2003a; Neubauer et al. 2012), there are also reports that peptidyl transfer to tmRNA occurs robustly even in the absence of EF-Tu

(Hallier et al. 2004; Shimizu and Ueda 2006). We asked how EF-Tu affects the rate of peptidyl transfer to tmRNA in our pre-steady state assays. We determined rates of peptidyl transfer to tmRNA with wild-type and His136Ala SmpB in the presence or absence of EF-Tu (Fig. 16B and 16C). Peptidyl transfer does occur in the absence of EF-Tu, as reported (Hallier et al. 2004; Shimizu and Ueda 2006), but we find that the rate is ~1000-fold slower for both SmpB constructs. We conclude that delivery of the tmRNA-SmpB complex by EF-Tu dramatically accelerates peptidyl transfer.

We next asked if release of the tmRNA-SmpB complex from EF-Tu into the A site occurs by the canonical conformational changes in EF-Tu that follow GTP hydrolysis or by an alternative mechanism. We blocked release of tmRNA by adding kirromycin to stalled ribosome complexes. Kirromycin binds EF-Tu, locking it in its GTP-bound conformation and preventing release of canonical aminoacylated tRNAs (Vogeley et al. 2001). As expected, in a control reaction, the rate of peptidyl transfer to Phe-tRNA^{Phe} was inhibited more than 3000-fold in the presence of kirromycin (Fig. 16A). When EF-Tu complexed with tmRNA and wild-type SmpB was reacted in the presence of kirromycin, the rate of peptidyl transfer was reduced by about 40-fold. This result shows that release from EF-Tu is important for licensing tmRNA reactivity (Fig. 16B), although to a lesser extent than observed with Phe-tRNA^{Phe}. When the His136Ala mutant was used, kirromycin only reduced the rate of peptidyl transfer two-fold (Fig. 16C). These results suggest that release of tmRNA from EF-Tu occurs in a manner that is less sensitive to kirromycin and can be decoupled from GTP hydrolysis.

mRNA length discrimination occurs after GTP hydrolysis

Given the unusual nature of GTP hydrolysis upon binding of the tmRNA-SmpB complex to the ribosome, we wondered what effect the mRNA length has on EF-Tu activation. To avoid interfering with productive protein synthesis, tmRNA is thought to react slowly or not at all with nascent peptides within ribosomes with intact mRNA templates. Indeed, an earlier report showed that peptidyl transfer to tmRNA was blocked by the presence of mRNA in the A site (Ivanova et al. 2004). These longer mRNAs are expected to be bound tightly in the mRNA channel formed by ribosome proteins S3, S4, and S5; they are just at the edge of the protected footprint of translating ribosomes as determined by toeprinting studies. The crystal structure shows the SmpB tail binding the in mRNA channel, forming a helix; the presence of mRNA in the channel would block this important interaction.

We determined GTP hydrolysis rates upon tmRNA-SmpB binding to initiation complexes containing a series of mRNA constructs of different length, with 0, 9, 15, or 21 nt downstream of the P-site codon. Unexpectedly, we found that GTP hydrolysis rates remained unchanged even as the mRNA length increased (Fig. 17A). To see if this was an artifact

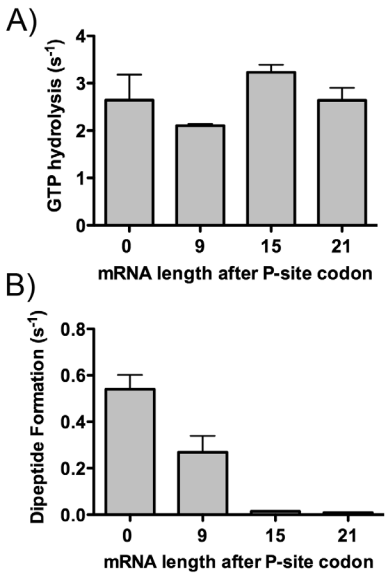

Figure 17. mRNA length has no effect on GTP hydorlysis by EF-Tu during ribosome rescue.

Peptidyl transfer (A) and GTP hydrolysis (B) rates were determined with the reaction of quaternary complex with ribosome initiation complexes containing mRNAs of varying lengths downstream of the P site: +0 nt, +9 nt, +15 nt, and +21 nt. Standard error is given.

of our mRNA templates or assay conditions, we recapitulated the peptidyl transfer rate data from the earlier study. As expected, peptidyl transfer rates to tmRNA were markedly slower in ribosome complexes with long mRNAs (Fig. 17B). The rates for the +15 and +21 nt mRNAs were particularly slow, more than 40-fold down. Taken together, these data show that discrimination of mRNA length by tmRNA and SmpB occurs after GTP hydrolysis by EF-Tu.

DISCUSSION

Stalled ribosomes accept Ala-tmRNA into the A site in the absence of a codon-anticodon interaction. Structural and biochemical studies show that tmRNA's protein partner, SmpB, binds the decoding center in the 30S A site (Kaur et al. 2006; Kurita et al. 2007; Nonin-Lecomte et al. 2009; Neubauer et al. 2012) . Although the C-terminal tail of SmpB is essential for peptidyl transfer to tmRNA (Sundermeier et al. 2005; Kurita et al. 2010; Miller et al. 2011), it was not thought to play a role in EF-Tu activation. In the present study, we have clarified the role of the SmpB tail in licensing tmRNA entry into stalled ribosomes, showing that it is critical for both EF-Tu activation and peptidyl transfer.

In canonical decoding, interactions between the conserved 16S rRNA nucleotides A1492, A1493, and G530 and the codon-anticodon helix effect global conformational changes in the ribosome that stimulate GTP hydrolysis by EF-Tu. In the crystal structure of *T. thermophilus* EF-Tu, SmpB, and tmRNA bound to the 70S ribosome and trapped in the A/T state with kirromycin, conserved residues in SmpB bind near these rRNA nucleotides in the decoding center. Mutation of positively-charged residues in helix 1 (data not shown)

or mutation of A1492 or A1493 had no significant effect on SmpB activity (Miller et al. 2011). This result is consistent with the fact that the residues in helix 1 are not in close contact with the bases of A1492 and A1493 in the crystal structure; potential hydrogen bonds are roughly 4 Å in length. It seems unlikely that these interactions are essential for SmpB function.

In contrast, our kinetic data strongly support the finding of Ramakrishnan and co-workers that the His136 side chain stacks on the G530 base (Neubauer et al. 2012). His136 mutants that are incapable of stacking have dramatically lower GTP hydrolysis rates, indicating that this interaction is essential for EF-Tu activation. These findings help explain why residue 136 is conserved as His or Tyr, two residues with high base-stacking propensities. Notably, although the aromatic Phe side chain is capable of participating in base-stacking interactions, the His136Phe mutant is inactive. This loss of activity may be due to lower stacking energy, as nucleobases stack more poorly with Phe than with His or Tyr (Rutledge et al. 2007), but we cannot rule out a possible requirement for hydrogen bonding to the hydroxyl group in Tyr or the imidazole moiety in His. Mutation of His136 to Ala or deletion of the C-terminal tail after residue 132 does not affect the affinity of SmpB for the ribosomal A site. Though the tail apparently contributes little to overall SmpB binding energy, we speculate that His136 alters the conformation of G530, leading to conformational changes similar to those observed in the canonical decoding process. Indeed, the *T. thermophilus* structure shows that the tmRNA-SmpB complex induces the closure of the 30S subunit observed in canonical decoding.

In a previous study, we found that ribosomes containing the 16S rRNA mutation G530A supported normal rates of peptidyl transfer and GTP hydrolysis by EF-Tu (Miller et al. 2011). Given that His136's interaction with G530 is through base stacking, it is not surprising that the G530A mutation does not reduce GTP hydrolysis rates because the stacking energies of His with guanine or adenine are similar (Rutledge et al. 2007). As the stacking energy between His and uracil is predicted to be significantly weaker, one might expect more of a reduction in the GTP hydrolysis rate in the G530U mutant than we observed. In combination with the His136Tyr SmpB mutant, however, the activity of the G530U ribosomes was substantially reduced. This synergistic defect is consistent with a mechanism in which both mutants (G530U and His136Tyr) are defective at the same step. We speculate that this GTPase activation is robust because binding and positioning of G530 and His136 is aided both by the nearby residues Lys138 and Arg139 in the D_{137}KR sequence and by interaction with the downstream portion of the C-terminal tail with the mRNA channel.

While our data offer a clear picture of how EF-Tu is activated by the tmRNA-SmpB complex, they also raise questions about the role of EF-Tu and GTP hydrolysis during *trans*-translation. Although early biochemical studies indicated that tmRNA binds to EF-Tu (Barends et al. 2000; Barends et al. 2001; Zvereva et al. 2001), and structures of complexes containing tmRNA, SmpB, EF-Tu, and 70S ribosomes were obtained (Valle et al. 2003a; Neubauer et al. 2012), there were also reports that peptidyl transfer to tmRNA could occur efficiently in the absence of EF-Tu (Hallier et al. 2004; Shimizu and Ueda 2006). In these two studies, peptidyl transfer to tmRNA occurred robustly over long reaction times without EF-Tu or with kirromycin. Our kinetic data resolve this discrepancy by showing that EF-Tu

is essential for rapid peptidyl transfer but that a similar endpoint is reached at long reaction times. Presumably by interacting with L7/L12, EF-Tu delivers the tmRNA-SmpB complex into the A site faster than it can bind on its own.

While EF-Tu's delivery of tmRNA to the A site is critical, it appears that GTP hydrolysis can be decoupled from peptidyl transfer to tmRNA. To our surprise, the His136Ala mutation in SmpB did not affect peptidyl transfer, though it reduced the rate of GTP hydrolysis ~70-fold. As a result of this single mutation in SmpB, the rate of GTPase activation is 30-fold slower than the rate of peptidyl transfer. The fact that GTP hydrolysis is not rate-limiting indicates the His136Ala mutant acts via an alternative mechanism, releasing the tmRNA-SmpB complex from EF-Tu without GTP hydrolysis. Note that in the case of wild-type SmpB, however, GTP hydrolysis may still occur prior to peptidyl transfer, as the rates are $3.4 \pm 1.2\ s^{-1}$ and $1.5 \pm 0.2\ s^{-1}$ respectively.

It appears that the tmRNA-SmpB complex is more easily released from EF-Tu for accommodation into the A site and peptidyl transfer than canonical tRNA is. Kirromycin binds EF-Tu and blocks conformational changes after GTP hydrolysis, trapping aminoacyl-tRNAs onto EF-Tu. Kirromycin slowed peptidyl transfer to Phe-tRNA more than 1000-fold, but only slowed peptidyl transfer to tmRNA by ~40-fold. These data are consistent with early reports that EF-Tu binds to Ala-tmRNA weaker than it binds Ala-tRNA (Barends et al. 2000; Barends et al. 2001). This lower affinity may contribute to facile tmRNA release from EF-Tu into the A site. In support of this idea, a mutation in EF-Tu that lowers its affinity for otherwise tight-binding aminoacyl-tRNAs increases the peptidyl-transfer rate because release from EF-Tu occurs more rapidly in the A site (Schrader et al. 2011).

Remarkably, the His136Ala mutant is only inhibited ~2-fold by kirromycin, suggesting that the tmRNA-SmpB complex is released from EF-Tu without the canonical conformational changes following GTP hydrolysis. We speculate that the His136Ala mutation alters the reaction pathway through changing SmpB's interactions with the ribosome and not by changing the dynamics of the EF-Tu complex. His136 is located near the junction of the C-terminal tail and the body of SmpB, far away from the tmRNA-binding site, making it unlikely that the tmRNA-SmpB interaction is compromised by this mutation. tmRNA binding to EF-Tu is not affected by SmpB (Barends et al. 2001), nor is there evidence of any contact between the C-terminal tail and EF-Tu in the crystal structure (Neubauer et al. 2012), arguing that the His136Ala mutation does not alter the binding of tmRNA and SmpB to EF-Tu. The simplest explanation is that its effects derive from the loss of the interaction of His136 and G530.

Contacts between the large tmRNA molecule and the ribosome may also partially explain the ability of tmRNA to undergo peptidyl transfer without inducing GTP hydrolysis. Measuring the endpoint of the peptidyl-transfer reaction to full-length tmRNA at 30 min, Ueda and co-workers found that peptidyl transfer occurred equally well in the absence or presence of EF-Tu and that kirromycin had no effect. In contrast, EF-Tu was essential for peptidyl transfer to a truncated tmRNA containing only the tRNA-like domain (TLD) and that the reaction was blocked by kirromycin (Shimizu and Ueda 2006). Their results raise the possibility that the body of tmRNA, consisting of four pseudoknots and the mRNA-like region, is at least partially responsible for tmRNA's unusual ability to undergo peptidyl transfer independently of EF-Tu, GTP hydrolysis, or in the presence of kirromycin.

In general terms, it makes biological sense that EF-Tu activation is less important for *trans*-translation than for canonical translation. In the latter, GTP hydrolysis separates two reversible tRNA selection steps, both essential for translational fidelity. In the former, codon selectivity per se is not involved, though tmRNA needs to selectively bind stalled ribosomes to avoid aborting productive protein synthesis. The length of mRNA after the A site codon determines which ribosomes tmRNA reacts with: peptidyl transfer to tmRNA is inhibited by the presence of mRNA in the channel downstream of the A site codon (Ivanova et al. 2004). In collaboration with Himeno and co-workers, we have found that GTP hydrolysis does not depend on mRNA length (Fig. 17). It seems that there is no discrimination against tmRNA prior to GTP hydrolysis, only after. Although EF-Tu delivers the tmRNA-SmpB complex to the ribosome and hydrolyzes GTP in the process, GTP hydrolysis does not separate key selection steps as it does in canonical decoding.

In conclusion, our working model of the initial steps of *trans*-translation is as follows: EF-Tu delivers SmpB and Ala-tmRNA to the ribosomal A site. The body of SmpB is responsible for its binding affinity in the decoding center. His136 stacks on G530 as positioned by D_{137}KR and other tail residues. GTP is hydrolyzed and tmRNA is released from EF-Tu, though it is not clear that GTP hydrolysis is always necessary. If the C-terminal tail can enter the mRNA channel, the tmRNA-SmpB complex is accommodated fully into the A site and peptidyl transfer takes place. If the mRNA length downstream of the A site codon is prohibitively long (9 nt or more), then the tmRNA-SmpB complex cannot accommodate properly and dissociates from the ribosome.

ACKNOWLEDGEMENTS

The authors thank Megan McDonald-Gilmore and Kristin Smith-Koutmou for assistance with the fluorescence experiments and Daisuke Kurita Hyouta Himeno for providing the SmpB tail peptide and valuable comments and criticism. This work was supported by NIH grant GM77633.

MATERIALS AND METHODS

Purification of translation components

Wild-type and G530U MS2-tagged ribosomes were expressed and purified as described (Youngman and Green 2005; Cochella et al. 2007; Miller et al. 2011). IF1, IF2, IF3, and His-tagged EF-Tu, PheRS, and AlaRS were purified as described (Shimizu et al. 2001; Cochella and Green 2005; Brunelle et al. 2006). Wild-type and mutant SmpB proteins were expressed and purified as described (Miller et al. 2011). Formyl-[^{35}S]Met-tRNA^{fMet} was prepared as described (Walker and Fredrick 2008). The mRNA GGAAUUCGGGCCCUUGUUAACAAUUAAGGAGGUAUACUAUGUUC was synthesized by T7 transcription of a template assembled by annealing sense and antisense oligonucleotides. It has a Phe codon in the A site with nothing downstream so that when incorporated into initiation complexes, it can react with either tmRNA-SmpB or Phe-tRNA^{Phe}. The mRNAs +0, +9, +15, and +21 were also synthesized as described above. tmRNA was synthesized and aminoacylated as described (Miller et al. 2011). The extent of tmRNA aminoacylation was 50%–60% as determined by a small parallel reaction with [^{14}C]-alanine. tRNA^{Phe} (Sigma) was aminoacylated with purified PheRS.

GTP hydrolysis reactions

70S initiation complexes and ternary and tmRNA-SmpB quaternary complexes were formed essentially as described (Miller et al. 2011). Initiation complexes were diluted to 400 nM prior to storage at −80 °C. GTP hydrolysis rate reactions were carried out on a KinTek RQF-3 quench-flow instrument at 20 °C. Equal volumes of initiation complexes and either ternary or quaternary complexes were rapidly mixed and quenched with 40% formic acid at the desired times. Inhibition by the synthetic peptide corresponding to the C-terminal tail (133-160) of SmpB was performed by incubating 500 μM synthetic peptide with the initiation complex before mixing with ternary or quaternary complexes. Reaction products were resolved on PEI cellulose TLC plates in 0.5 M KH_2PO_4 (pH 3.5) and analyzed by autoradiography. The data were fit to a first-order equation with GraphPad Prism5 software. All reported reactions were performed at least twice and the standard error is given.

Peptide-bond formation reactions

70S initiation complexes were formed as described (Miller et al. 2011). The Phe-$tRNA^{Phe}$ ternary complex was prepared by incubating 5 μM charged Phe-$tRNA^{Phe}$, 20 μM EF-Tu, and 1 mM GTP in buffer A (50 mM Tris-HCl pH 7.5, 70 mM NH_4Cl, 30 mM KCl, 7 mM $MgCl_2$, and 1 mM dithiothreitol). The tmRNA-SmpB quaternary complexes were prepared by incubating 5 μM charged tmRNA (~10 μM total), 20 μM SmpB, and 1 mM GTP in buffer A

on ice for 5 min; 20 μM EF-Tu was added, and the reaction mixture was incubated for 15 min on ice.

Peptide-bond formation rate reactions were carried out at 20 °C by mixing equal volumes of initiation complexes with either ternary or quaternary complexes. Inhibition by kirromycin was performed by incubating 200 μM kirromycin with the initiation complexes before mixing with ternary or quaternary complexes. Inhibition by the synthetic peptide was performed as described above. The reactions were stopped at the desired times by addition of KOH to a final concentration of 0.3 M. Reactions with relatively fast rate constants (>0.05 sec^{-1}) were performed on the KinTek RQF-3 quench-flow instrument. Reaction products were resolved using cellulose TLC plates in pyridine acetate (pH 2.8) as described (Youngman et al. 2004) and analyzed by autoradiography. The data were fit to a first-order equation with GraphPad Prism5 software. All reported reactions were performed at least twice, and the standard error is given.

Fluorescence measurements

$tRNA^{Phe}$ was labeled with proflavin by resuspending 100 μM $tRNA^{Phe}$ in 50 mM Tris-HCl, pH 7.5 and 10 mg/ml $NaBH_4$ (in 10 mM KOH). After incubating at 0 °C for 1 h, the $tRNA^{Phe}$ was precipitated with ethanol and resuspended in 0.1 M NaOAc pH 4.2. The $tRNA^{Phe}$ was incubated with 30 mM proflavin at 37 °C for 16 h. Excess proflavin was removed by phenol/chloroform extraction followed by ethanol precipitation. The labeled $tRNA^{Phe}$ was resuspended in water and aminoacylated as described above.

Labeled ribosome complexes were assembled by incubating 2 μM 70S ribosomes, 6 μM mRNA, 3 μM fMet-tRNA^{fMet}, 3 μM each IF1, IF2, and IF3, and 2 mM GTP in buffer A at 37°C for 45 min. Ternary complex containing labeled Phe-tRNA^{Phe} were made by incubating 20 μM EF-Tu, 2 μM labeled Phe-tRNAPhe, 1.6 mM GTP, and 2 μM EF-G in buffer A on ice for 15 min. The ribosome initiation complex and ternary complex were mixed and allowed to incubate for 10 min at 37 °C. The labeled complex was purified by layering over a 1.3-mL sucrose cushion (1.1 M sucrose, 20 mM Tris-HCl at pH 7.5, 500 mM NH_4Cl, 10 mM $MgCl_2$, 0.5 mM EDTA) and spun at 258,000g in a TLA100.3 rotor for 2 h. The resulting pellet was resuspended in buffer A and stored at −80 °C.

Fluorescence measurements were performed on a Fluorolog-3 spectrofluorometer (Horiba). The excitation wavelength was 449 nm. Emission spectra were obtained as SmpB at desired concentrations was added to 5 nM labeled ribosome complexes.

REFERENCES

Abo T, Inada T, Ogawa K, Aiba H. 2000. SsrA-mediated tagging and proteolysis of LacI and its role in the regulation of lac operon. *Embo J* **19**: 3762-3769.

Andersen ES, Rosenblad MA, Larsen N, Westergaard JC, Burks J, Wower IK, Wower J, Gorodkin J, Samuelsson T, Zwieb C. 2006. The tmRDB and SRPDB resources. *Nucleic Acids Res* **34**: D163-168.

Barends S, Karzai AW, Sauer RT, Wower J, Kraal B. 2001. Simultaneous and functional binding of SmpB and EF-Tu-TP to the alanyl acceptor arm of tmRNA. *J Mol Biol* **314**: 9-21.

Barends S, Wower J, Kraal B. 2000. Kinetic parameters for tmRNA binding to alanyl-tRNA synthetase and elongation factor Tu from Escherichia coli. *Biochemistry-Us* **39**: 2652-2658.

Bernstein JA, Khodursky AB, Lin PH, Lin-Chao S, Cohen SN. 2002. Global analysis of mRNA decay and abundance in Escherichia coli at single-gene resolution using two-color fluorescent DNA microarrays. *Proc Natl Acad Sci U S A* **99**: 9697-9702.

Bessho Y, Shibata R, Sekine S, Murayama K, Higashijima K, Hori-Takemoto C, Shirouzu M, Kuramitsu S, Yokoyama S. 2007. Structural basis for functional mimicry of long-variable-arm tRNA by transfer-messenger RNA. *Proc Natl Acad Sci U S A* **104**: 8293-8298.

Bjornsson A, Isaksson LA. 1996. Accumulation of a mRNA decay intermediate by ribosomal pausing at a stop codon. *Nucleic Acids Res* **24**: 1753-1757.

Blanchard SC, Gonzalez RL, Kim HD, Chu S, Puglisi JD. 2004. tRNA selection and kinetic proofreading in translation. *Nature structural & molecular biology* **11**: 1008-1014.

Brunelle JL, Youngman EM, Sharma D, Green R. 2006. The interaction between C75 of tRNA and the A loop of the ribosome stimulates peptidyl transferase activity. *Rna* **12**: 33-39.

Bugaeva EY, Shpanchenko OV, Felden B, Isaksson LA, Dontsova OA. 2008. One SmpB molecule accompanies tmRNA during its passage through the ribosomes. *FEBS Lett* **582**: 1532-1536.

Chadani Y, Ono K, Ozawa S, Takahashi Y, Takai K, Nanamiya H, Tozawa Y, Kutsukake K, Abo T. 2010. Ribosome rescue by Escherichia coli ArfA (YhdL) in the absence of trans-translation system. *Mol Microbiol* **78**: 796-808.

Chauhan AK, Apirion D. 1989. The gene for a small stable RNA (10Sa RNA) of Escherichia coli. *Mol Microbiol* **3**: 1481-1485.

Cheng K, Ivanova N, Scheres SH, Pavlov MY, Carazo JM, Hebert H, Ehrenberg M, Lindahl M. 2010. tmRNA.SmpB complex mimics native aminoacyl-tRNAs in the A site of stalled ribosomes. *J Struct Biol* **169**: 342-348.

Choy JS, Aung LL, Karzai AW. 2007. Lon protease degrades transfer-messenger RNA-tagged proteins. *J Bacteriol* **189**: 6564-6571.

Cochella L, Brunelle JL, Green R. 2007. Mutational analysis reveals two independent molecular requirements during transfer RNA selection on the ribosome. *Nature structural & molecular biology* **14**: 30-36.

Cochella L, Green R. 2005. An active role for tRNA in decoding beyond codon:anticodon pairing. *Science* **308**: 1178-1180.

Cole C, Barber JD, Barton GJ. 2008. The Jpred 3 secondary structure prediction server. *Nucleic Acids Res* **36**: W197-201.
Collier J, Bohn C, Bouloc P. 2004. SsrA tagging of Escherichia coli SecM at its translation arrest sequence. *J Biol Chem* **279**: 54193-54201.
Condon C. 2007. Maturation and degradation of RNA in bacteria. *Curr Opin Microbiol* **10**: 271-278.
Crooks GE, Hon G, Chandonia JM, Brenner SE. 2004. WebLogo: a sequence logo generator. *Genome Res* **14**: 1188-1190.
Daviter T, Gromadski KB, Rodnina MV. 2006. The ribosome's response to codon-anticodon mismatches. *Biochimie* **88**: 1001-1011.
Diaconu M, Kothe U, Schlunzen F, Fischer N, Harms JM, Tonevitsky AG, Stark H, Rodnina MV, Wahl MC. 2005. Structural basis for the function of the ribosomal L7/12 stalk in factor binding and GTPase activation. *Cell* **121**: 991-1004.
Dong G, Nowakowski J, Hoffman DW. 2002. Structure of small protein B: the protein component of the tmRNA-SmpB system for ribosome rescue. *EMBO J* **21**: 1845-1854.
Dulebohn D, Choy J, Sundermeier T, Okan N, Karzai AW. 2007. Trans-translation: The tmRNA-mediated surveillance mechanism for ribosome rescue, directed protein degradation, and nonstop mRNA decay. *Biochemistry-Us* **46**: 4681-4693.
Farrell CM, Grossman AD, Sauer RT. 2005. Cytoplasmic degradation of ssrA-tagged proteins. *Mol Microbiol* **57**: 1750-1761.
Felden B, Hanawa K, Atkins JF, Himeno H, Muto A, Gesteland RF, McCloskey JA, Crain PF. 1998. Presence and location of modified nucleotides in Escherichia coli tmRNA: structural mimicry with tRNA acceptor branches. *EMBO J* **17**: 3188-3196.
Felden B, Himeno H, Muto A, McCutcheon JP, Atkins JF, Gesteland RF. 1997. Probing the structure of the Escherichia coli 10Sa RNA (tmRNA). *RNA* **3**: 89-103.
Flynn JM, Levchenko I, Seidel M, Wickner SH, Sauer RT, Baker TA. 2001. Overlapping recognition determinants within the ssrA degradation tag allow modulation of proteolysis. *Proc Natl Acad Sci U S A* **98**: 10584-10589.
Fu J, Hashem Y, Wower I, Lei J, Liao HY, Zwieb C, Wower J, Frank J. 2010. Visualizing the transfer-messenger RNA as the ribosome resumes translation. *EMBO J* **29**: 3819-3825.
Garza-Sanchez F, Gin JG, Hayes CS. 2008. Amino acid starvation and colicin D treatment induce A-site mRNA cleavage in Escherichia coli. *J Mol Biol* **378**: 505-519.
Garza-Sanchez F, Janssen BD, Hayes CS. 2006. Prolyl-tRNA(Pro) in the A-site of SecM-arrested ribosomes inhibits the recruitment of transfer-messenger RNA. *J Biol Chem* **281**: 34258-34268.
Garza-Sanchez F, Shoji S, Fredrick K, Hayes CS. 2009. RNase II is important for A-site mRNA cleavage during ribosome pausing. *Mol Microbiol* **73**: 882-897.
Gillet R, Kaur S, Li W, Hallier M, Felden B, Frank J. 2007. Scaffolding as an organizing principle in trans-translation. The roles of small protein B and ribosomal protein S1. *J Biol Chem* **282**: 6356-6363.
Gottesman S, Roche E, Zhou Y, Sauer RT. 1998. The ClpXP and ClpAP proteases degrade proteins with carboxy-terminal peptide tails added by the SsrA-tagging system. *Genes Dev* **12**: 1338-1347.

Gromadski KB, Rodnina MV. 2004. Kinetic determinants of high-fidelity tRNA discrimination on the ribosome. *Mol Cell* **13**: 191-200.
Gutmann S, Haebel PW, Metzinger L, Sutter M, Felden B, Ban N. 2003. Crystal structure of the transfer-RNA domain of transfer-messenger RNA in complex with SmpB. *Nature* **424**: 699-703.
Hallier M, Desreac J, Felden B. 2006. Small protein B interacts with the large and the small subunits of a stalled ribosome during trans-translation. *Nucleic Acids Research* **34**: 1935-1943.
Hallier M, Ivanova N, Rametti A, Pavlov M, Ehrenberg M, Felden B. 2004. Pre-binding of small protein B to a stalled ribosome triggers trans-translation. *Journal of Biological Chemistry* **279**: 25978-25985.
Hanawa-Suetsugu K, Bordeau V, Himeno H, Muto A, Felden B. 2001. Importance of the conserved nucleotides around the tRNA-like structure of Escherichia coli transfer-messenger RNA for protein tagging. *Nucleic Acids Res* **29**: 4663-4673.
Hanawa-Suetsugu K, Takagi M, Inokuchi H, Himeno H, Muto A. 2002. SmpB functions in various steps of trans-translation. *Nucleic Acids Res* **30**: 1620-1629.
Hartmann RK, Gossringer M, Spath B, Fischer S, Marchfelder A. 2009. The making of tRNAs and more - RNase P and tRNase Z. *Prog Mol Biol Transl Sci* **85**: 319-368.
Hayes CS, Bose B, Sauer RT. 2002a. Proline residues at the C terminus of nascent chains induce SsrA tagging during translation termination. *J Biol Chem* **277**: 33825-33832.
-. 2002b. Stop codons preceded by rare arginine codons are efficient determinants of SsrA tagging in Escherichia coli. *Proc Natl Acad Sci U S A* **99**: 3440-3445.
Hayes CS, Sauer RT. 2003. Cleavage of the A site mRNA codon during ribosome pausing provides a mechanism for translational quality control. *Mol Cell* **12**: 903-911.
Herman C, Thevenet D, Bouloc P, Walker GC, D'Ari R. 1998. Degradation of carboxy-terminal-tagged cytoplasmic proteins by the Escherichia coli protease HflB (FtsH). *Genes Dev* **12**: 1348-1355.
Holberger LE, Hayes CS. 2009. Ribosomal protein S12 and aminoglycoside antibiotics modulate A-site mRNA cleavage and transfer-messenger RNA activity in Escherichia coli. *J Biol Chem* **284**: 32188-32200.
Hong SJ, Tran QA, Keiler KC. 2005. Cell cycle-regulated degradation of tmRNA is controlled by RNase R and SmpB. *Mol Microbiol* **57**: 565-575.
Hou YM, Schimmel P. 1988. A simple structural feature is a major determinant of the identity of a transfer RNA. *Nature* **333**: 140-145.
Huang C, Wolfgang MC, Withey J, Koomey M, Friedman DI. 2000. Charged tmRNA but not tmRNA-mediated proteolysis is essential for Neisseria gonorrhoeae viability. *Embo J* **19**: 1098-1107.
Hutchison CA, Peterson SN, Gill SR, Cline RT, White O, Fraser CM, Smith HO, Venter JC. 1999. Global transposon mutagenesis and a minimal Mycoplasma genome. *Science* **286**: 2165-2169.
Ivanov PV, Zvereva MI, Shpanchenko OV, Dontsova OA, Bogdanov AA, Aglyamova GV, Lim VI, Teraoka Y, Nierhaus KH. 2002. How does tmRNA move through the ribosome? *FEBS Lett* **514**: 55-59.
Ivanova N, Lindell M, Pavlov M, Holmberg Schiavone L, Wagner EG, Ehrenberg M. 2007. Structure probing of tmRNA in distinct stages of trans-translation. *RNA* **13**: 713-722.

Ivanova N, Pavlov MY, Ehrenberg M. 2005. tmRNA-induced release of messenger RNA from stalled ribosomes. *J Mol Biol* **350**: 897-905.
Ivanova N, Pavlov MY, Felden B, Ehrenberg M. 2004. Ribosome rescue by tmRNA requires truncated mRNAs. *J Mol Biol* **338**: 33-41.
Jacob Y, Sharkady SM, Bhardwaj K, Sanda A, Williams KP. 2005. Function of the SmpB tail in transfer-messenger RNA translation revealed by a nucleus-encoded form. *Journal of Biological Chemistry* **280**: 5503-5509.
Janssen BD, Hayes CS. 2012. The tmRNA ribosome-rescue system. *Adv Protein Chem Struct Biol* **86**: 151-191.
Julio SM, Heithoff DM, Mahan MJ. 2000. ssrA (tmRNA) plays a role in Salmonella enterica serovar Typhimurium pathogenesis. *J Bacteriol* **182**: 1558-1563.
Karzai AW, Sauer RT. 2001. Protein factors associated with the SsrA.SmpB tagging and ribosome rescue complex. *Proc Natl Acad Sci U S A* **98**: 3040-3044.
Karzai AW, Susskind MM, Sauer RT. 1999. SmpB, a unique RNA-binding protein essential for the peptide-tagging activity of SsrA (tmRNA). *EMBO J* **18**: 3793-3799.
Kaur S, Gillet R, Li W, Gursky R, Frank J. 2006. Cryo-EM visualization of transfer messenger RNA with two SmpBs in a stalled ribosome. *Proc Natl Acad Sci U S A* **103**: 16484-16489.
Keiler KC. 2008. Biology of trans-translation. *Annu Rev Microbiol* **62**: 133-151.
Keiler KC, Waller PR, Sauer RT. 1996. Role of a peptide tagging system in degradation of proteins synthesized from damaged messenger RNA. *Science* **271**: 990-993.
Komine Y, Kitabatake M, Yokogawa T, Nishikawa K, Inokuchi H. 1994. A tRNA-like structure is present in 10Sa RNA, a small stable RNA from Escherichia coli. *Proc Natl Acad Sci U S A* **91**: 9223-9227.
Konno T, Kurita D, Takada K, Muto A, Himeno H. 2007. A functional interaction of SmpB with tmRNA for determination of the resuming point of trans-translation. *RNA* **13**: 1723-1731.
Kothe U, Wieden HJ, Mohr D, Rodnina MV. 2004. Interaction of helix D of elongation factor Tu with helices 4 and 5 of protein L7/12 on the ribosome. *J Mol Biol* **336**: 1011-1021.
Kurita D, Muto A, Himeno H. 2010. Role of the C-terminal tail of SmpB in the early stage of trans-translation. *RNA* **16**: 980-990.
Kurita D, Sasaki R, Muto A, Himeno H. 2007. Interaction of SmpB with ribosome from directed hydroxyl radical probing. *Nucleic Acids Research* **35**: 7248-7255.
Lee S, Ishii M, Tadaki T, Muto A, Himeno H. 2001. Determinants on tmRNA for initiating efficient and precise trans-translation: some mutations upstream of the tag-encoding sequence of Escherichia coli tmRNA shift the initiation point of trans-translation in vitro. *Rna* **7**: 999-1012.
Levchenko I, Seidel M, Sauer RT, Baker TA. 2000. A specificity-enhancing factor for the ClpXP degradation machine. *Science* **289**: 2354-2356.
Li X, Hirano R, Tagami H, Aiba H. 2006. Protein tagging at rare codons is caused by tmRNA action at the 3' end of nonstop mRNA generated in response to ribosome stalling. *Rna* **12**: 248-255.
Li Z, Deutscher MP. 2002. RNase E plays an essential role in the maturation of Escherichia coli tRNA precursors. *RNA* **8**: 97-109.

Li Z, Pandit S, Deutscher MP. 1998. 3' exoribonucleolytic trimming is a common feature of the maturation of small, stable RNAs in Escherichia coli. *Proc Natl Acad Sci U S A* **95**: 2856-2861.
Lies M, Maurizi MR. 2008. Turnover of endogenous SsrA-tagged proteins mediated by ATP-dependent proteases in Escherichia coli. *J Biol Chem* **283**: 22918-22929.
Lin-Chao S, Wei CL, Lin YT. 1999. RNase E is required for the maturation of ssrA RNA and normal ssrA RNA peptide-tagging activity. *Proc Natl Acad Sci U S A* **96**: 12406-12411.
Loomis WP, Koo JT, Cheung TP, Moseley SL. 2001. A tripeptide sequence within the nascent DaaP protein is required for mRNA processing of a fimbrial operon in Escherichia coli. *Mol Microbiol* **39**: 693-707.
Luo P, Baldwin RL. 1997. Mechanism of helix induction by trifluoroethanol: a framework for extrapolating the helix-forming properties of peptides from trifluoroethanol/water mixtures back to water. *Biochemistry-Us* **36**: 8413-8421.
Makarov EM, Apirion D. 1992. 10Sa RNA: processing by and inhibition of RNase III. *Biochem Int* **26**: 1115-1124.
Marshall RA, Aitken CE, Dorywalska M, Puglisi JD. 2008. Translation at the single-molecule level. *Annual review of biochemistry* **77**: 177-203.
McClain WH, Foss K. 1988. Changing the identity of a tRNA by introducing a G-U wobble pair near the 3' acceptor end. *Science* **240**: 793-796.
McClain WH, Guerrier-Takada C, Altman S. 1987. Model substrates for an RNA enzyme. *Science* **238**: 527-530.
McGinness KE, Sauer RT. 2004. Ribosomal protein S1 binds mRNA and tmRNA similarly but plays distinct roles in translation of these molecules. *Proc Natl Acad Sci U S A* **101**: 13454-13459.
Mehta P, Richards J, Karzai AW. 2006. tmRNA determinants required for facilitating nonstop mRNA decay. *RNA* **12**: 2187-2198.
Metzinger L, Hallier M, Felden B. 2005. Independent binding sites of small protein B onto transfer-messenger RNA during trans-translation. *Nucleic Acids Res* **33**: 2384-2394.
-. 2008. The highest affinity binding site of small protein B on transfer messenger RNA is outside the tRNA domain. *RNA* **14**: 1761-1772.
Miller MR, Healey DW, Robison SG, Dewey JD, Buskirk AR. 2008. The role of upstream sequences in selecting the reading frame on tmRNA. *BMC biology* **6**: 29.
Miller MR, Liu Z, Cazier DJ, Gebhard GM, Herron SR, Zaher HS, Green R, Buskirk AR. 2011. The role of SmpB and the ribosomal decoding center in licensing tmRNA entry into stalled ribosomes. *RNA* **17**: 1727-1736.
Moazed D, Noller HF. 1991. Sites of interaction of the CCA end of peptidyl-tRNA with 23S rRNA. *Proc Natl Acad Sci U S A* **88**: 3725-3728.
Moore SD, Sauer RT. 2005. Ribosome rescue: tmRNA tagging activity and capacity in Escherichia coli. *Mol Microbiol* **58**: 456-466.
-. 2007. The tmRNA system for translational surveillance and ribosome rescue. *Annual review of biochemistry* **76**: 101-124.
Murzin AG. 1993. OB(oligonucleotide/oligosaccharide binding)-fold: common structural and functional solution for non-homologous sequences. *EMBO J* **12**: 861-867.

Muto A, Fujihara A, Ito KI, Matsuno J, Ushida C, Himeno H. 2000. Requirement of transfer-messenger RNA for the growth of Bacillus subtilis under stresses. *Genes Cells* **5**: 627-635.
Nakatogawa H, Ito K. 2002. The ribosomal exit tunnel functions as a discriminating gate. *Cell* **108**: 629-636.
Nameki N, Chattopadhyay P, Himeno H, Muto A, Kawai G. 1999a. An NMR and mutational analysis of an RNA pseudoknot of Escherichia coli tmRNA involved in trans-translation. *Nucleic Acids Res* **27**: 3667-3675.
Nameki N, Felden B, Atkins JF, Gesteland RF, Himeno H, Muto A. 1999b. Functional and structural analysis of a pseudoknot upstream of the tag-encoded sequence in E. coli tmRNA. *J Mol Biol* **286**: 733-744.
Nameki N, Someya T, Okano S, Suemasa R, Kimoto M, Hanawa-Suetsugu K, Terada T, Shirouzu M, Hirao I, Takaku H et al. 2005. Interaction analysis between tmRNA and SmpB from Thermus thermophilus. *J Biochem* **138**: 729-739.
Nameki N, Tadaki T, Himeno H, Muto A. 2000. Three of four pseudoknots in tmRNA are interchangeable and are substitutable with single-stranded RNAs. *FEBS Lett* **470**: 345-349.
Nameki N, Tadaki T, Muto A, Himeno H. 1999c. Amino acid acceptor identity switch of Escherichia coli tmRNA from alanine to histidine in vitro. *J Mol Biol* **289**: 1-7.
Neubauer C, Gao YG, Andersen KR, Dunham CM, Kelley AC, Hentschel J, Gerdes K, Ramakrishnan V, Brodersen DE. 2009. The structural basis for mRNA recognition and cleavage by the ribosome-dependent endonuclease RelE. *Cell* **139**: 1084-1095.
Neubauer C, Gillet R, Kelley AC, Ramakrishnan V. 2012. Decoding in the absence of a codon by tmRNA and SmpB in the ribosome. *Science* **335**: 1366-1369.
Nonin-Lecomte S, Germain-Amiot N, Gillet R, Hallier M, Ponchon L, Dardel F, Felden B. 2009. Ribosome hijacking: a role for small protein B during trans-translation. *EMBO Rep* **10**: 160-165.
O'Connor M. 2007. Minimal translation of the tmRNA tag-coding region is required for ribosome release. *Biochemical and biophysical research communications* **357**: 276-281.
Ogle JM, Brodersen DE, Clemons WM, Jr., Tarry MJ, Carter AP, Ramakrishnan V. 2001. Recognition of cognate transfer RNA by the 30S ribosomal subunit. *Science* **292**: 897-902.
Ogle JM, Murphy FV, Tarry MJ, Ramakrishnan V. 2002. Selection of tRNA by the ribosome requires a transition from an open to a closed form. *Cell* **111**: 721-732.
Ogle JM, Ramakrishnan V. 2005. Structural insights into translational fidelity. *Annual review of biochemistry* **74**: 129-177.
Oh BK, Apirion D. 1991. 10Sa RNA, a small stable RNA of Escherichia coli, is functional. *Mol Gen Genet* **229**: 52-56.
Oh BK, Chauhan AK, Isono K, Apirion D. 1990. Location of a gene (ssrA) for a small, stable RNA (10Sa RNA) in the Escherichia coli chromosome. *J Bacteriol* **172**: 4708-4709.
Okan NA, Bliska JB, Karzai AW. 2006. A Role for the SmpB-SsrA system in Yersinia pseudotuberculosis pathogenesis. *PLoS Pathog* **2**: e6.
Pape T, Wintermeyer W, Rodnina M. 1999. Induced fit in initial selection and proofreading of aminoacyl-tRNA on the ribosome. *Embo J* **18**: 3800-3807.

Pedersen K, Zavialov AV, Pavlov MY, Elf J, Gerdes K, Ehrenberg M. 2003. The bacterial toxin RelE displays codon-specific cleavage of mRNAs in the ribosomal A site. *Cell* **112**: 131-140.
Powers T, Noller HF. 1990. Dominant lethal mutations in a conserved loop in 16S rRNA. *Proc Natl Acad Sci U S A* **87**: 1042-1046.
Qi H, Shimizu Y, Ueda T. 2007. Ribosomal protein S1 is not essential for the trans-translation machinery. *J Mol Biol* **368**: 845-852.
Ramadoss NS, Alumasa JN, Cheng L, Wang Y, Li S, Chambers BS, Chang H, Chatterjee AK, Brinker A, Engels IH et al. 2013. Small molecule inhibitors of trans-translation have broad-spectrum antibiotic activity. *Proceedings of the National Academy of Sciences*.
Ramakrishnan V. 2002. Ribosome Structure and the Mechanism of Translation. *Cell* **108**: 557-572.
Richards J, Mehta P, Karzai AW. 2006. RNase R degrades non-stop mRNAs selectively in an SmpB-tmRNA-dependent manner. *Mol Microbiol* **62**: 1700-1712.
Roche ED, Sauer RT. 1999. SsrA-mediated peptide tagging caused by rare codons and tRNA scarcity. *EMBO J* **18**: 4579-4589.
-. 2001. Identification of endogenous SsrA-tagged proteins reveals tagging at positions corresponding to stop codons. *J Biol Chem* **276**: 28509-28515.
Rodnina MV, Pape T, Fricke R, Kuhn L, Wintermeyer W. 1996. Initial binding of the elongation factor Tu.GTP.aminoacyl-tRNA complex preceding codon recognition on the ribosome. *J Biol Chem* **271**: 646-652.
Rodnina MV, Wintermeyer W. 2001. Fidelity of aminoacyl-tRNA selection on the ribosome: kinetic and structural mechanisms. *Annual review of biochemistry* **70**: 415-435.
Rudinger-Thirion J, Giege R, Felden B. 1999. Aminoacylated tmRNA from Escherichia coli interacts with prokaryotic elongation factor Tu. *RNA* **5**: 989-992.
Rutledge LR, Campbell-Verduyn LS, Wetmore SD. 2007. Characterization of the stacking interactions between DNA or RNA nucleobases and the aromatic amino acids. *Chemical Physics Letters* **444**: 167-175.
Ruusala T, Ehrenberg M, Kurland CG. 1982. Is there proofreading during polypeptide synthesis? *EMBO J* **1**: 741-745.
Saguy M, Gillet R, Skorski P, Hermann-Le Denmat S, Felden B. 2007. Ribosomal protein S1 influences trans-translation in vitro and in vivo. *Nucleic Acids Res* **35**: 2368-2376.
Schluenzen F, Tocilj A, Zarivach R, Harms J, Gluehmann M, Janell D, Bashan A, Bartels H, Agmon I, Franceschi F et al. 2000. Structure of functionally activated small ribosomal subunit at 3.3 angstroms resolution. *Cell* **102**: 615-623.
Schmeing TM, Voorhees RM, Kelley AC, Gao YG, Murphy FVt, Weir JR, Ramakrishnan V. 2009. The crystal structure of the ribosome bound to EF-Tu and aminoacyl-tRNA. *Science* **326**: 688-694.
Schrader JM, Chapman SJ, Uhlenbeck OC. 2011. Tuning the affinity of aminoacyl-tRNA to elongation factor Tu for optimal decoding. *Proc Natl Acad Sci U S A* **108**: 5215-5220.
Schuette JC, Murphy FVt, Kelley AC, Weir JR, Giesebrecht J, Connell SR, Loerke J, Mielke T, Zhang W, Penczek PA et al. 2009. GTPase activation of elongation factor EF-Tu by the ribosome during decoding. *EMBO J* **28**: 755-765.
Selinger DW, Saxena RM, Cheung KJ, Church GM, Rosenow C. 2003. Global RNA half-life analysis in Escherichia coli reveals positional patterns of transcript degradation. *Genome Res* **13**: 216-223.

Selmer M, Dunham CM, Murphy FVt, Weixlbaumer A, Petry S, Kelley AC, Weir JR, Ramakrishnan V. 2006. Structure of the 70S ribosome complexed with mRNA and tRNA. *Science* **313**: 1935-1942.

Shimizu Y, Inoue A, Tomari Y, Suzuki T, Yokogawa T, Nishikawa K, Ueda T. 2001. Cell-free translation reconstituted with purified components. *Nature biotechnology* **19**: 751-755.

Shimizu Y, Ueda T. 2002. The role of SmpB protein in trans-translation. *FEBS Lett* **514**: 74-77.

-. 2006. SmpB triggers GTP hydrolysis of elongation factor Tu on ribosomes by compensating for the lack of codon-anticodon interaction during trans-translation initiation. *Journal of Biological Chemistry* **281**: 15987-15996.

Shpanchenko OV, Zvereva MI, Ivanov PV, Bugaeva EY, Rozov AS, Bogdanov AA, Kalkum M, Isaksson LA, Nierhaus KH, Dontsova OA. 2005. Stepping transfer messenger RNA through the ribosome. *Journal of Biological Chemistry* **280**: 18368-18374.

Someya T, Nameki N, Hosoi H, Suzuki S, Hatanaka H, Fujii M, Terada T, Shirouzu M, Inoue Y, Shibata T et al. 2003. Solution structure of a tmRNA-binding protein, SmpB, from Thermus thermophilus. *FEBS Lett* **535**: 94-100.

Srivastava RK, Miczak A, Apirion D. 1990. Maturation of precursor 10Sa RNA in Escherichia coli is a two-step process: the first reaction is catalyzed by RNase III in presence of Mn2+. *Biochimie* **72**: 791-802.

Stark H, Rodnina MV, Wieden HJ, Zemlin F, Wintermeyer W, van Heel M. 2002. Ribosome interactions of aminoacyl-tRNA and elongation factor Tu in the codon-recognition complex. *Nature structural biology* **9**: 849-854.

Sundermeier TR, Dulebohn DP, Cho HJ, Karzai AW. 2005. A previously uncharacterized role for small protein B (SmpB) in transfer messenger RNA-mediated trans-translation. *Proc Natl Acad Sci U S A* **102**: 2316-2321.

Sundermeier TR, Karzai AW. 2007. Functional SmpB-ribosome interactions require tmRNA. *Journal of Biological Chemistry* **282**: 34779-34786.

Sunohara T, Jojima K, Tagami H, Inada T, Aiba H. 2004a. Ribosome stalling during translation elongation induces cleavage of mRNA being translated in Escherichia coli. *J Biol Chem* **279**: 15368-15375.

Sunohara T, Jojima K, Yamamoto Y, Inada T, Aiba H. 2004b. Nascent-peptide-mediated ribosome stalling at a stop codon induces mRNA cleavage resulting in nonstop mRNA that is recognized by tmRNA. *Rna* **10**: 378-386.

Takada K, Takemoto C, Kawazoe M, Konno T, Hanawa-Suetsugu K, Lee S, Shirouzu M, Yokoyama S, Muto A, Himeno H. 2007. In vitro trans-translation of Thermus thermophilus: ribosomal protein S1 is not required for the early stage of trans-translation. *Rna* **13**: 503-510.

Tanner DR, Cariello DA, Woolstenhulme CJ, Broadbent MA, Buskirk AR. 2009. Genetic identification of nascent peptides that induce ribosome stalling. *J Biol Chem* **284**: 34809-34818.

Tanner DR, Dewey JD, Miller MR, Buskirk AR. 2006. Genetic analysis of the structure and function of transfer messenger RNA pseudoknot 1. *J Biol Chem* **281**: 10561-10566.

Thibonnier M, Thiberge JM, De Reuse H. 2008. Trans-translation in Helicobacter pylori: essentiality of ribosome rescue and requirement of protein tagging for stress resistance and competence. *PLoS One* **3**: e3810.

Thompson RC, Stone PJ. 1977. Proofreading of the codon-anticodon interaction on ribosomes. *Proc Natl Acad Sci U S A* **74**: 198-202.
Tu GF, Reid GE, Zhang JG, Moritz RL, Simpson RJ. 1995. C-terminal extension of truncated recombinant proteins in Escherichia coli with a 10Sa RNA decapeptide. *J Biol Chem* **270**: 9322-9326.
Valle M, Gillet R, Kaur S, Henne A, Ramakrishnan V, Frank J. 2003a. Visualizing tmRNA entry into a stalled ribosome. *Science* **300**: 127-130.
Valle M, Zavialov A, Li W, Stagg SM, Sengupta J, Nielsen RC, Nissen P, Harvey SC, Ehrenberg M, Frank J. 2003b. Incorporation of aminoacyl-tRNA into the ribosome as seen by cryo-electron microscopy. *Nature structural biology* **10**: 899-906.
Vogeley L, Palm GJ, Mesters JR, Hilgenfeld R. 2001. Conformational change of elongation factor Tu (EF-Tu) induced by antibiotic binding. Crystal structure of the complex between EF-Tu.GDP and aurodox. *The Journal of biological chemistry* **276**: 17149-17155.
Walker SE, Fredrick K. 2008. Preparation and evaluation of acylated tRNAs. *Methods (San Diego, Calif* **44**: 81-86.
Watson JD. 2008. Molecular biology of the gene / James D. Watson ... [et al.]. Vol 6th ed. San Francisco : Pearson/Benjamin Cummings ; Cold Spring Harbor, N.Y. : Cold Spring Harbor Laboratory Press, c2008.
Watts T, Cazier D, Healey D, Buskirk A. 2009. SmpB contributes to reading frame selection in the translation of transfer-messenger RNA. *J Mol Biol* **391**: 275-281.
Weis F, Bron P, Giudice E, Rolland JP, Thomas D, Felden B, Gillet R. 2010a. tmRNA-SmpB: a journey to the centre of the bacterial ribosome. *EMBO J* **29**: 3810-3818.
Weis F, Bron P, Rolland JP, Thomas D, Felden B, Gillet R. 2010b. Accommodation of tmRNA-SmpB into stalled ribosomes: a cryo-EM study. *RNA* **16**: 299-306.
Williams KP. 2000. The tmRNA website. *Nucleic Acids Res* **28**: 168.
Williams KP, Bartel DP. 1996. Phylogenetic analysis of tmRNA secondary structure. *RNA* **2**: 1306-1310.
Williams KP, Martindale KA, Bartel DP. 1999. Resuming translation on tmRNA: a unique mode of determining a reading frame. *EMBO J* **18**: 5423-5433.
Wower IK, Zwieb C, Wower J. 2004. Contributions of pseudoknots and protein SmpB to the structure and function of tmRNA in trans-translation. *J Biol Chem* **279**: 54202-54209.
-. 2009. Escherichia coli tmRNA lacking pseudoknot 1 tags truncated proteins in vivo and in vitro. *RNA* **15**: 128-137.
Wower IK, Zwieb CW, Guven SA, Wower J. 2000. Binding and cross-linking of tmRNA to ribosomal protein S1, on and off the Escherichia coli ribosome. *Embo J* **19**: 6612-6621.
Wower J, Zwieb CW, Hoffman DW, Wower IK. 2002. SmpB: a protein that binds to double-stranded segments in tmRNA and tRNA. *Biochemistry-Us* **41**: 8826-8836.
Yamamoto Y, Sunohara T, Jojima K, Inada T, Aiba H. 2003. SsrA-mediated trans-translation plays a role in mRNA quality control by facilitating degradation of truncated mRNAs. *RNA* **9**: 408-418.
Yao S, Blaustein JB, Bechhofer DH. 2008. Erythromycin-induced ribosome stalling and RNase J1-mediated mRNA processing in Bacillus subtilis. *Mol Microbiol* **69**: 1439-1449.

Youngman EM, Brunelle JL, Kochaniak AB, Green R. 2004. The active site of the ribosome is composed of two layers of conserved nucleotides with distinct roles in peptide bond formation and peptide release. *Cell* **117**: 589-599.
Youngman EM, Green R. 2005. Affinity purification of in vivo-assembled ribosomes for in vitro biochemical analysis. *Methods (San Diego, Calif* **36**: 305-312.
Yusupova GZ, Yusupov MM, Cate JH, Noller HF. 2001. The path of messenger RNA through the ribosome. *Cell* **106**: 233-241.
Zaher HS, Green R. 2009a. Fidelity at the Molecular Level: Lessons from Protein Synthesis. *Cell* **136**: 746-762.
Zaher HS, Green R. 2009b. Quality control by the ribosome following peptide bond formation. *Nature* **457**: 161-166.
Zvereva MI, Ivanov PV, Teraoka Y, Topilina NI, Dontsova OA, Bogdanov AA, Kalkum M, Nierhaus KH, Shpanchenko OV. 2001. Complex of transfer-messenger RNA and elongation factor Tu. Unexpected modes of interaction. *J Biol Chem* **276**: 47702-47708.
Zwieb C, Wower J. 2000. tmRDB (tmRNA database). *Nucleic Acids Res* **28**: 169-170.